# PNEUMACTIVE

# A SOFT, CUSTOMIZABLE, RESPONSIVE SHADING DEVICE DESIGN FOR ENRICHED USER EXPERIENCE IN PUBLIC SPACES

A Thesis

Presented to the Faculty of the Graduate School

of Cornell University

In Partial Fulfillment of the Requirements for the Degree of

Master of Science in Matter Design Computation

by

Yifei Peng

May 2022

# ABSTRACT

Responsive or active shading devices feature various designs that enable automated adjustments to enhance performance in environmental conditioning. However, existing solutions mostly yield high cost and demand complex installation while featuring minimal support for convenient customization.

Pneumactive is a prototypical exploration of the performance, usability, and aesthetics of pneumatic actuator and membrane assemblies towards soft, modular, affordable, and customizable responsive shading device designs. The transformable system is achieved by programming the internal structures (strain limiters) of each actuator and compositions of actuators and membranes suspended among them.

An automated control system was designed to enable not only explorations of the morphological behavior of the device with each component independently actuated to various levels, but also an opportunity to experiment with interaction programs based on a set of parameters including time intervals, light intensity, and distance to moving objects.

The thesis will demonstrate the iterative development process in actuator design, material testing, fabrication technique, and interaction study. The final prototype attempts to provide implications of the feasibility and usability for shading applications through a series of testing on a fully integrated device system.

This research will shed light on the potential applications of soft robotics in architecture while advancing concepts in material, fabrication, interaction study, and design for usability in the development of responsive architectural devices.

# BIOGRAPHICAL SKETCH

Yifei Peng was born in Zhenjiang city, Jiangsu Province, China. After completing his schoolwork at Faith Christian Academy in Poughkeepsie, New York in 2015, Yifei entered Rensselaer Polytechnic Institute in Troy, New York. He received a Bachelor of Architecture and a Master of Science in Communication and Rhetoric from Rensselaer Polytechnic Institute in May 2020. He entered the MatterDesignComputation graduate program at Cornell University during the following two years.

To my family

# ACKNOWLEDGMENTS

I would like to acknowledge and give my warmest thanks to my thesis advisor, Professor Jenny Sabin, who helped me start this project and guided me throughout all the stages of the research.

I would also like to thank my thesis advisory committee, Dr. Robert Shepherd, Dr. Jay Yoon, and Dr. Itai Cohen, for challenging my knowledge and guiding design directions as my thesis developed.

I would like to give special thanks to my parents for their unconditional love, support, and understanding.

TABLE OF CONTENTS

# CHAPTER 1

# INTRODUCTION

Responsive or active shading devices feature various designs that enable automated adjustments to enhance performance in environmental conditioning, energy-saving, and visual attraction in some design cases. However, existing mechanical solutions, including the predominant rotating shading systems mostly feature substantial structures, and yield high cost. Emerging solutions such as smart glazing systems demand less space, material, and modification to the existing building structure but require significantly higher initial cost (Al Dakheel, et al. 2017). While interior shading systems are more affordable, they generally exhibit less capability than exterior shading systems in reducing cooling loads (Ye,et al, 2016). More importantly, while capable of minor adjustment, existing offerings in responsive shading systems usually lack support for easy re-configuration by users, such as removing, adding, or relocating components, due to their substantial size and fixed mounting mechanism.

This becomes problematic, especially during the pandemic when people start to either work remotely or demand social distancing. The device would provide less utility in the first situation due to reduced occupants, and the resources could be used elsewhere. In the second situation, more indoor partitioning would be required for the occupants' wellbeing in the workplace.

This research seeks to fill this gap by offering design strategies for a responsive shading device that is affordable, deployable, configurable, and can also be used for partitioning purposes after simple adjustment. With the device's functionality being extended, it is given the opportunity to interact with both the environment and its users based on parameters beyond lighting and thermal conditions, so users can benefit from added features and enriched experiences. To reduce the initial and maintenance cost, a modular design approach was adopted to reduce the size and cost of each unit of the shading system while mitigating the scale of repair or replacement when necessary. A pneumatic actuation system was used to activate a series of soft actuators that expand and transform under pressure to provide adequate shading and partitioning functionalities. These interchangeable actuators developed in this research feature a wide range of transformability based on various internal structures programmed into each unit. One could easily arrange the composition of a set of actuators to accommodate parameters including sun angle, lighting intensity, required area coverage, and more. By replacing rigid mechanical structures and components with soft, extensible materials, the device can be better adapted to various spatial constraints and safer in case of an accident. In addition, the inflated actuators can serve as thermal insulators to improve their performance in environmental conditioning. The device can be easily aggregated or re-configured using the integrated magnetic attachment mechanism based on the modular design **(Figure 1)**.

This research will shed light on the potential applications of soft robotics in architecture while advancing concepts in material, fabrication, interaction study, and design for usability in the development of responsive architectural devices.

This thesis will first present relevant works in fields including responsive architectural devices, bio-inspired designs, inflatable structures, and soft actuators. Then, it will elaborate on the iterative development process in actuator design, material testing, fabrication technique, and interaction study. In the end, all designs and prototypes will be demonstrated and evaluated.

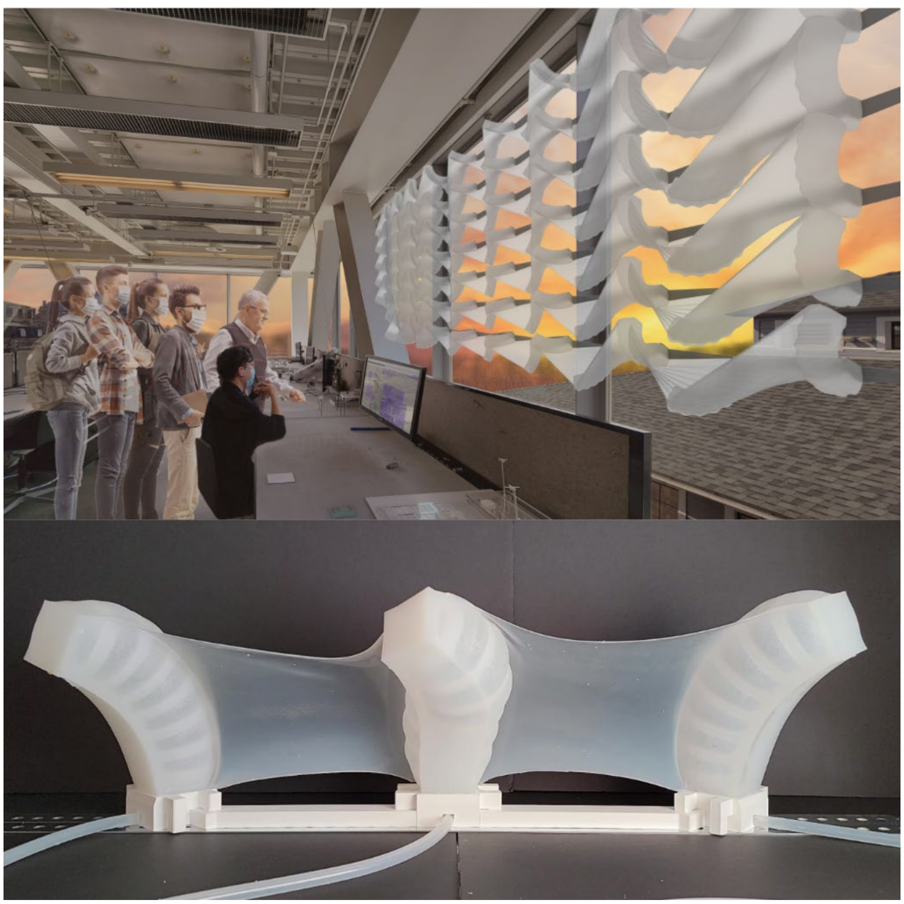

**Figure 1.** Design Concept

# CHAPTER 2

# BACKGROUND

### *Introduction*

To understand the context of this research and to explore potential design directions, a series of literature reviews were conducted, and relevant precedence is presented. This research first looked at designs of responsive architectural devices to understand various types of interaction and how they benefit users. Then, inflatable structures were investigated for their outstanding volume-weight ratio and simplicity in design and fabrication. To enable interaction based on physical transformation of an inflatable structure, this research studied projects utilizing soft actuators. Finally, topics on bio-inspired designs were reviewed to help generate the design concept.

### *Responsive Architectural device*

As building technology advances in material, structure, and the integration of electronic control systems, the built environment is getting more intelligent in improving energy efficiency, enhancing health and comfort for its inhabitants, and offering better support in usability, convenience, and accommodation to elevate the user experience. A crucial innovation that enables building intelligence is responsive and interactive architectural devices, which monitor changes in environmental conditions or human activities and kinetically make adjustments to the space.

In the 1970s, Nicolas Negroponte proposed integrating computing power into built spaces and structures to create responsive architecture capable of processing and reacting to recognition, intention, contextual variation, and meaning (d'Estrée Sterk, 2005). However, the design and programming of why, what, when, and how to respond to these environmental parameters and user demands truly distinguishes the built environment's intelligence. Therefore, concepts and designs of responsive architecture emerged and evolved long before the application of artificial intelligence and the Internet of Things (IoT). One of the forerunners in this field is Cedric Price. His Fun Palace proposal defined an adaptive building structural system that adjusts the configuration of circulations and enclosures embedded in a space frame superstructure to transform the spatial experience of architecture for its inhabitants radically. While the framework of this concept influenced the later design trend of "High Tech" architecture such as the Center Georges Pompidou in 1977, which featured visible expression of independence between structure, services, and skin, the actual implementation of adaptability encountered substantial challenges in both design and construction (Meagher, 2015). The concept of the kinetic modification of space has been further developed beyond its instrumentality using various approaches such as transformable building structure based on tensegrity space frames (d'Estrée Sterk, 2003), dynamic facade constructed using a matrix of pneumatic piston actuated metal plates (Aegis Hypo-Surface, dECOi) (Liu, 2002), building envelope formed by mist (Blur, Diller & Scofidio) (Diller, et al, 2002).

The other important design direction for responsive architecture is active environmental conditioning. Designs in this category are often programmed to kinetically respond to one or multiple environmental situations, including lighting control (Manzan, et al, 2017), solar thermal control, ventilation control, and more (Linn, 2014). Most existing solutions that utilize a mechanical system to achieve transformation can be divided into four types: the overhang, folding, horizontal louver, and vertical louver (Kensek, et al, 2011). Despite their extraordinary energy-saving and space conditioning performance, these devices usually demand high initial and maintenance costs, lack customization support, and require some degree of building modification. There have been studies on alternative solutions that use inexpensive materials and construction methods and are capable of customization. One example is the HygroSkin project, which utilizes the material-inherent behavior of thin plywood sheets in combination with computational programming and robotic fabrication to create responsive architectural devices based on passive hygroscopic actuation (Krieg, et al, 2014). While having significant advantages in cost, weight, and design flexibility, the durability and weather resistance of the device has yet to be improved.

Beyond kinetic spatial modification and environmental conditioning, some responsive architectural devices can also interact with human inhabitants through audiovisual communication. For example, Freshwater Pavilion by NOX uses an interactive program comprising projected animation, lighting, and audio to alter people's perception of space, thus creating a dynamic virtual environment responding to the behaviors of its users (Spybroek, et al, 1997). With the advancement in AI technologies, later projects such as Ada by Jenny Sabin Studio took this concept further by creating lighting responses to sentiment readings correlated with facial patterns, voice tones, and sound (Burry, et al, 2020). Interactions created using this approach often feature quicker response, better noticeability, and more design flexibility, thus carrying a higher level of intimacy to users and providing emotional support to some extent. While having many advantages in the effectiveness of interaction with human inhabitants, these designs usually feature a static physical structure and operate mainly in the perceptual dimension, restricting their potential applications in the field of physical environmental conditioning. Also, such systems usually yield high cost of entry and limited potential in the commercial market.

### *Inflatable Structures*

Inflatable structures have broad applications in architecture for their significant advantages in weight-saving, deployability, and ability to achieve complex surface designs for relatively low cost and effort compared to methods using wood catenary (Wong et al., 2019) or concrete casting (Schipper, 2016). However, most design approaches in inflatable structures based on single or double pressurized membranes employ inextensible materials that demand complicated, bespoke cut patterns. This constraint sets challenges in the design and fabrication of such structures, limiting the potential for generating more sophisticated geometries (Baranovskaya et al., 2016) and reducing the opportunity for mass production.

Projects such as PneuSystems attempt to address this issue by adopting a modular construction system. Cellular pneumatic membrane-based actuators are aggregated to form larger structural assemblies, and morphological variations can be achieved by controlling individual units' actuation and manipulating the composition (Velikov, 2014). While this approach enables standardization in manufacturing, The aggregation mechanism based on interlocking actuators sets restrictions on the range of transformation at both local and global scales. Another approach utilizes a composite material system comprising inflatable units and knitted boundaries to achieve scalability and design flexibility while maintaining a relatively efficient and stable structure (Baranovskaya et al., 2016). However, by adopting such a dualistic material system, the difficulty of precisely controlling the form during every stage of actuation exponentially increases.

Other studies attempt to work around this issue by segmenting the actuator body into assemblies of smaller units and using them as framing to shape suspended knitted surfaces (Wang et al., 2016). While this technique does increase the control of transformation in both individual actuators and the assembly, the tensile behavior of knitted fabrics imposes restrictions on the usable range of transformation.

### *Soft Actuator*

Advances in elastomeric materials and rapid prototyping techniques enable the rapid development of soft pneumatic actuators. Most soft actuator designs that aim to achieve flexing and extending behaviors feature structures inspired by nature. Similar to the human finger consisting of flexible joints and resistive tendons, these actuator designs mostly contain expandable chambers working against rigid backings to create bending (Souhail, et al, 2018). One example is the bellow shaped PneuNets structure, where a series of chambers are directly situated on the inextensible backing to enable rapid flexing under pneumatic pressure (Ilievski, et al, 2011). While these types of actuators are specialized in creating efficient locomotive behaviors (Shepherd, et al, 2011), they feature a negligible increase in volume through the range of transformation. One approach in using soft actuators to achieve surface texture morphing is to embed prefabricated strain-limiting elements into the actuator surface (Pikul et al., 2017). While this method carries significant advantages in creating non-standard surface structures, it lacks scalability to be used in architecture.

### *Bio-Inspired Designs*

This project also drew inspiration from bio-inspired robot designs. There have been a series of studies on pectoral fin locomotion utilized by sunfish, perch, bass, and bird wrasse (Moored, 2011), and recent devices attempt to replicate the actively flexible fins, construed based on the fin ray and connective membrane, which produce chordwise undulations as well as spanwise curvature (Yan, et al, 2010). Researchers also developed robotic devices based on other membrane structures in nature, such as a bat wing consisting of flexible bones and a highly anisotropic wing membrane featuring morphing capabilities (Colorado, 2012).

### *Conclusion*

These studies provided a foundational understanding of existing designs inside and outside of the architectural field, demonstrated challenges that must be addressed in this research, and revealed potential design directions that could be valuable. Based on the literature review, this research seeks to develop a responsive shading solution using soft actuators which transform under pneumatic pressure to achieve active environmental conditioning and user interaction.

# CHAPTER 3

# ACTUATOR DESIGN

### *Introduction*

Since the project aims to develop a shading/partition device based on inflatable soft actuators that transform when pressure is applied, a modular, aggregable envelope profile with pre-defined strain-limiting structures was used in the design. This chapter focuses on demonstrating the actuator designs evolved during the four iterations and elaborating the design considerations through the process.

### *Iteration One*

It was initially speculated that the final version of the actuator would be substantial in dimension, so the first iteration conducted material and structural studies on two typical portions of the final actuator: a flat diaphragm and a corner. The idea is to gather preliminary information from these two typical studies and then scale up to study the complete actuator.

Four types of structural programming were investigated in this iteration based on the negative correlation between surface thickness and expansion ratio at any given pressure level. The first one is simply modifying the thickness of the envelope surface to generate biased surface expansion when inflated. The second method is "bridging," which uses solid linking structures that directly attach to adjacent or opposing envelope surfaces to constrain the local surface expansion around the bridge. The third method is "bracing", which adds reinforcement members along the envelope surface, thus limiting the global expansion of the actuator. The fourth method is "serial channels", which break the envelope chamber into several smaller segments. By manipulating the placement of these small channels, both local and global transformation under pressure can be controlled **(Figure 2)**.


**Figure 2.** Actuator Structural Programming - First Iteration

***Iteration Two***

As the actuator fabrication progressed during the first iteration, the complexity of mold design and potential concerns for scalability started to indicate the inadequacy of the current design strategy. Therefore, the second iteration took a different approach by applying segmentation to the design and turned the speculated stand-alone large actuator profile into an assembly consisting of a series of smaller linear actuators and suspended membranes. Each of these linear actuators contains a set of “bracing” type of strain limiters lined up in its axial direction. These strain limiters would be programmed to generate differentiated local expansion, causing the whole actuator to transform under pressure. As the actuators inflate and transform, those membranes suspended among them would be stretched accordingly, creating new forms at the global scale **(Figure 3)**.

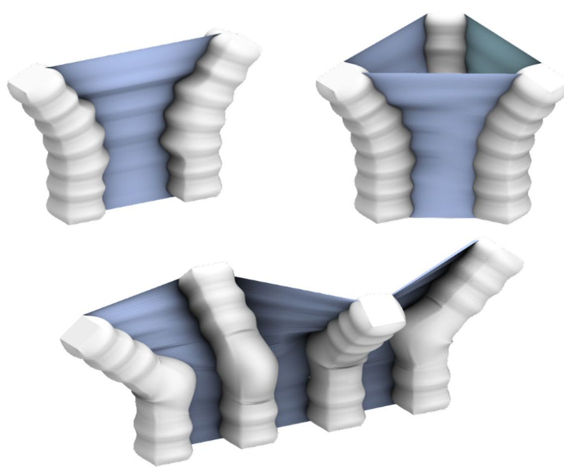

**Figure 3.** Actuator Design Concept - Second Iteration

Such actuator-membrane assembly can be activated to appropriate levels according to the external parameters such as the natural light condition to block and diffuse light entering the building interior **(Figure 4)**.

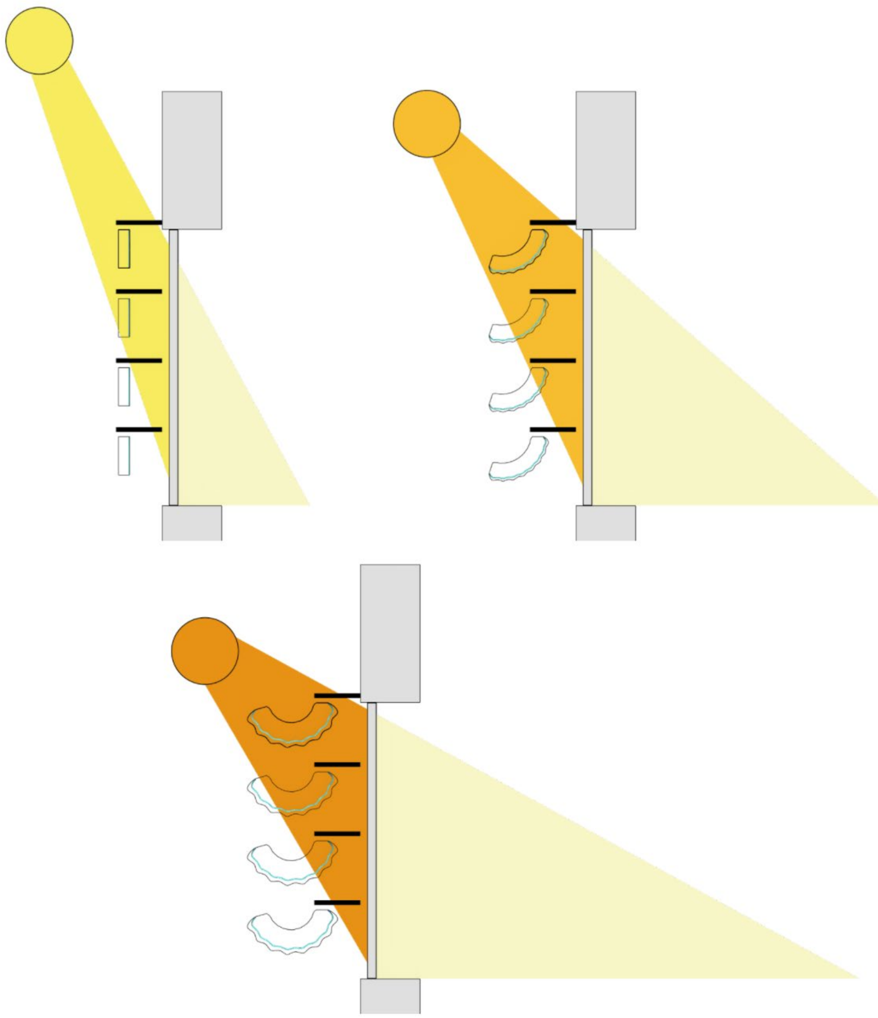

**Figure 4.** Function Definition - Second Iteration

Based on this concept, eight initial strain limiter programs were designed to achieve various types of transformations. By removing a portion of the radial strain limiter, that part of the actuator would expand more than the rest, causing the whole actuator to bend at the point of removal. Twisting is achieved by combining a series of points of bending in different directions. Also, it was suspected that a greater degree of bending would appear by condensing the strain limiter on the opposite side of a point of removal **(Figure 5)**.

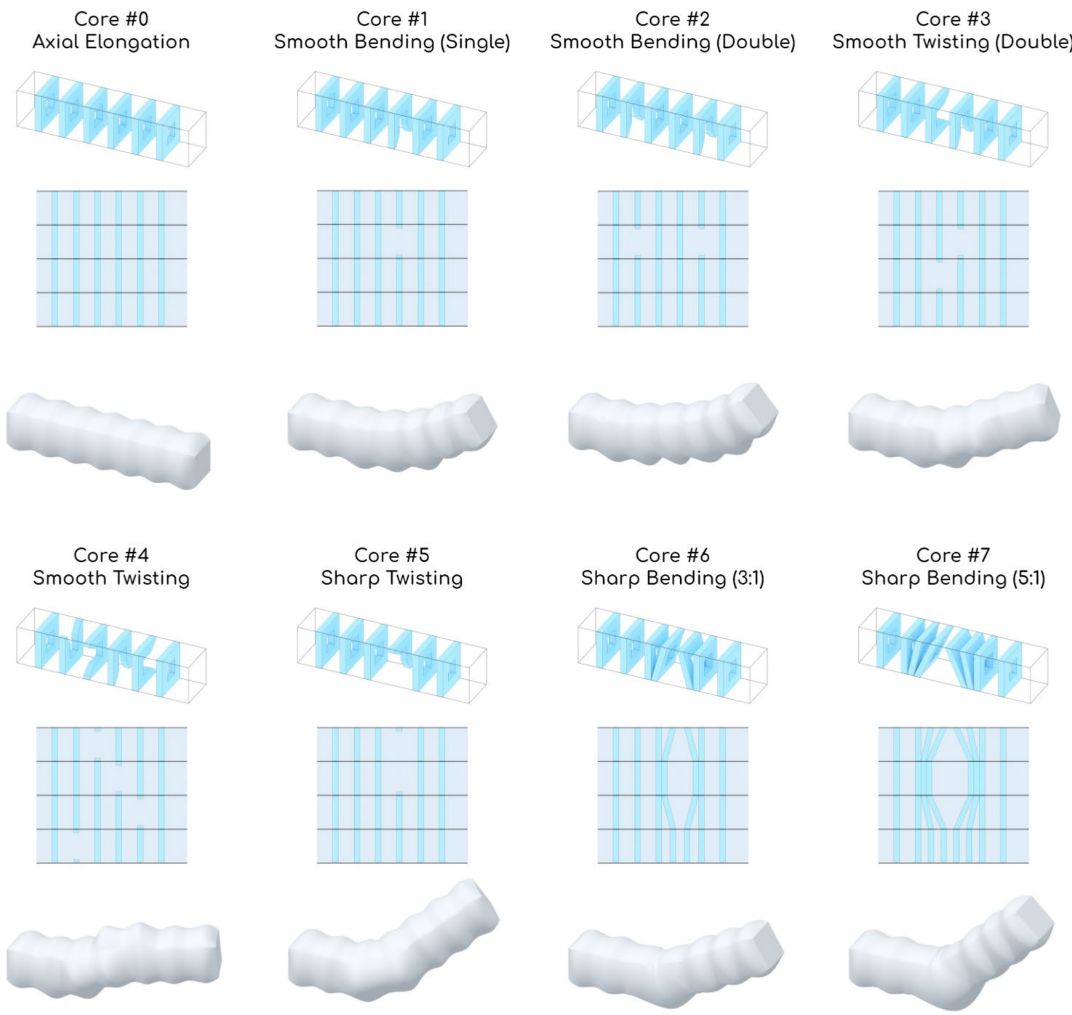


**Figure 5.** Actuator Structural Programming - Second Iteration

*Iteration Three*

Through the testing of actuator samples based on the second iteration of the design, it was found that removing segments from a single strain limiter made a limited impact on the global bending behavior of the actuator, sometimes even being undermined by fabrication inconsistencies. In addition, the condensing of strain limiters made demolding rather challenging. Therefore, the third iteration of the design identified three major types of strain limiter programs: extension (no removal), bulging (partial strain limiter removal), and bending (fusing multiple strain limiters into a solid backing) **(Figure 6)**.

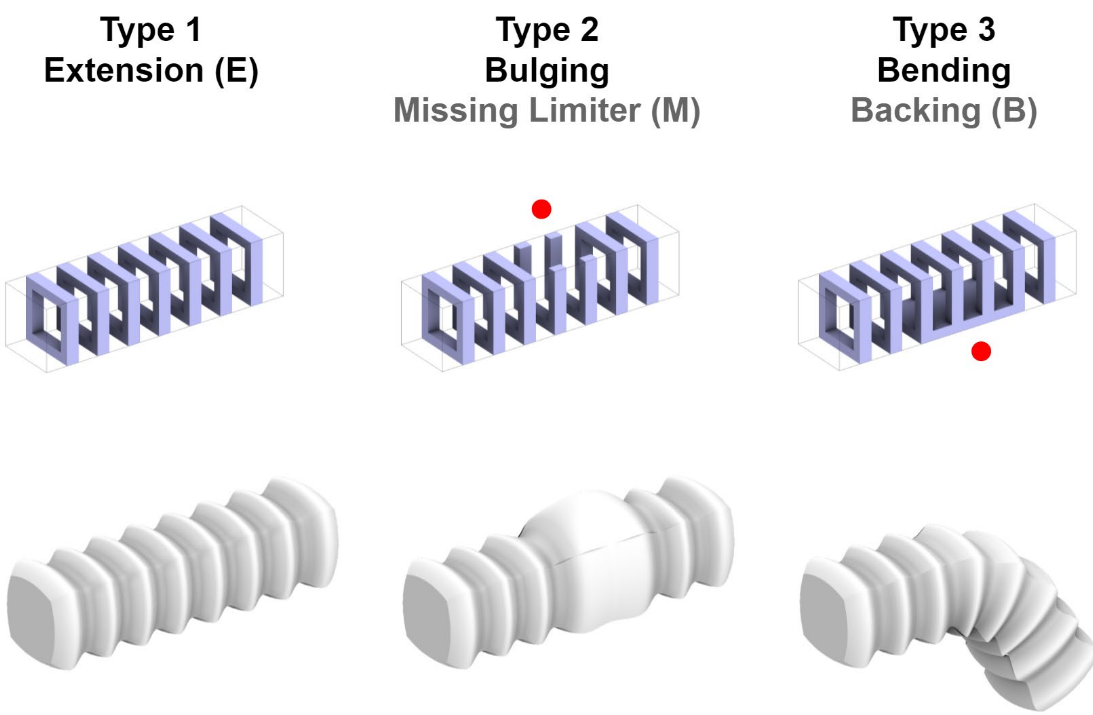


**Figure 6.** Actuator Design Concept - Third Iteration

By multiplying, combining, and altering these three types of strain limiter programs, 11 actuator structures were defined and fabricated for testing **(Figure 7)**.

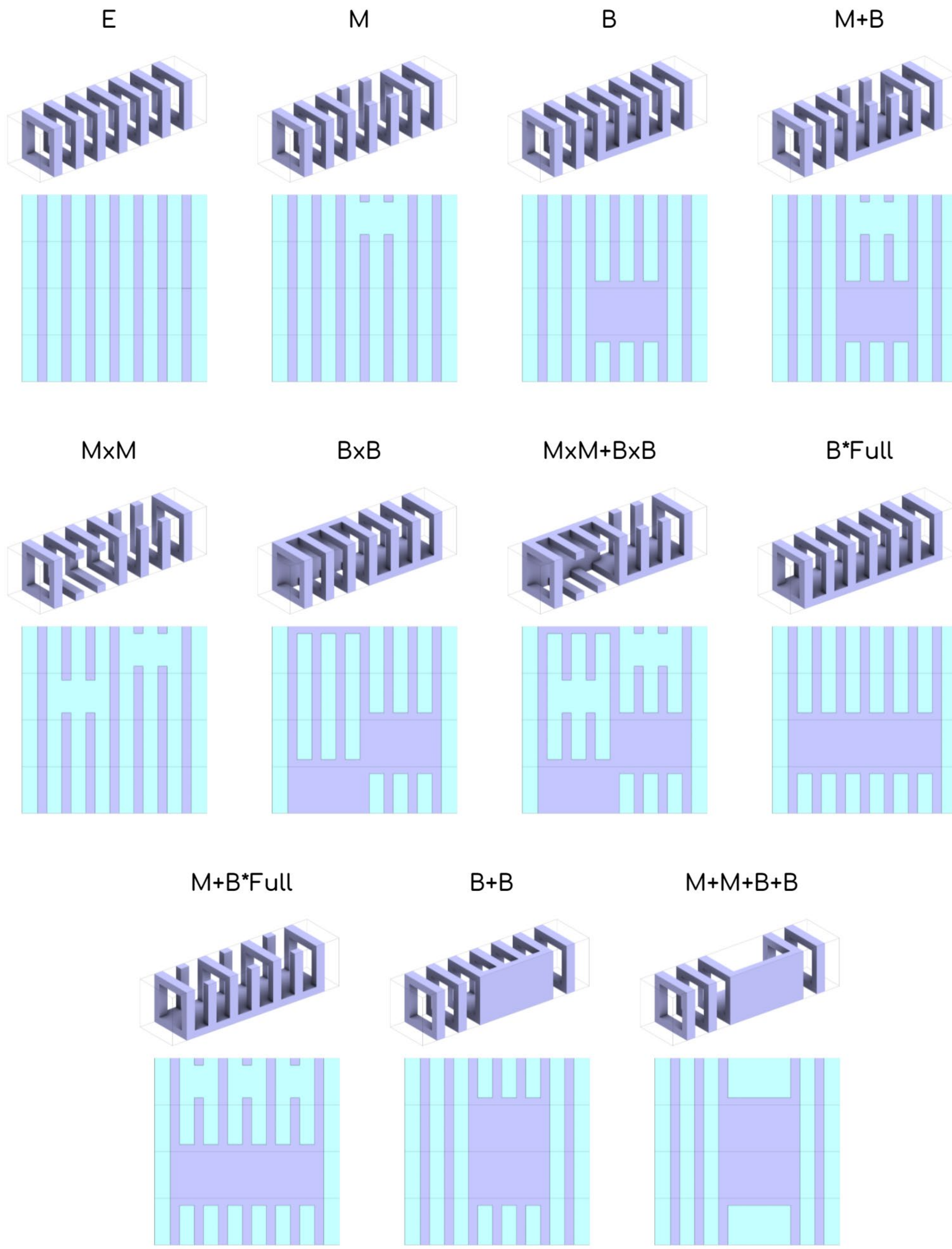


**Figure 7.** Actuator Structural Programming - Third Iteration

During this iteration, strain limiters and actuator sidewalls were fabricated independently using two different materials. The section profile of strain limiter inherited from the previous iteration was unable to provide enough contact surface at the point of lamination, causing the actuator structure to fall apart after demolding. To solve this problem, the strain limiter profile was revised to enhance the lamination **(Figure 8)**.

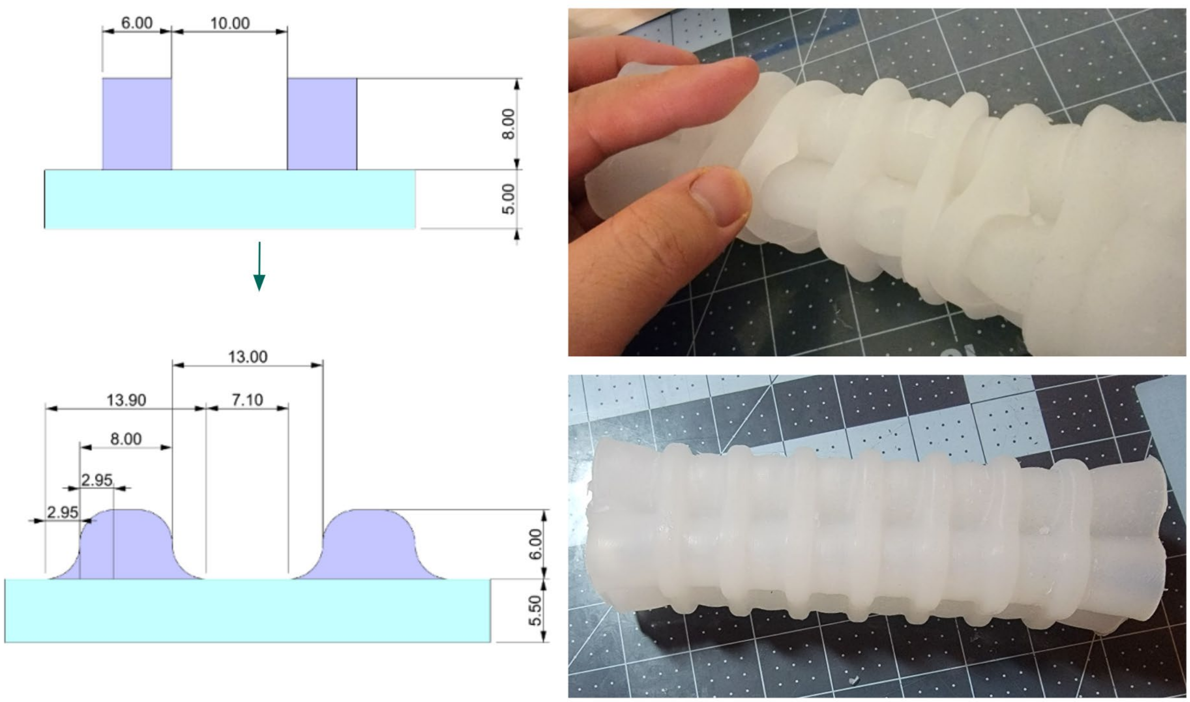


**Figure 8.** Actuator Strain Limiter Profile - Third Iteration

*Iteration Four*

Although the actuator samples based on the third design iteration received satisfactory testing results, occasional delamination between strain limiters and actuator sidewalls still occurred. The majority of those incidences were found at locations where the strain limiter was partially removed, leaving a single point of contact with the sidewall. The new strain limiter design no longer removes the whole segment to create an uneven surface expansion to overcome this issue. Instead, it only trims off the top portion of that strain limiter segment, leaving the bottom portion in contact with the actuator sidewall. In addition, the new strain limiter section profile featured a wider and thicker base to further enhance the lamination **(Figure 9)**. New samples fabricated based on the revised structure could sustain a significantly higher pressure without tearing or delamination during testing.

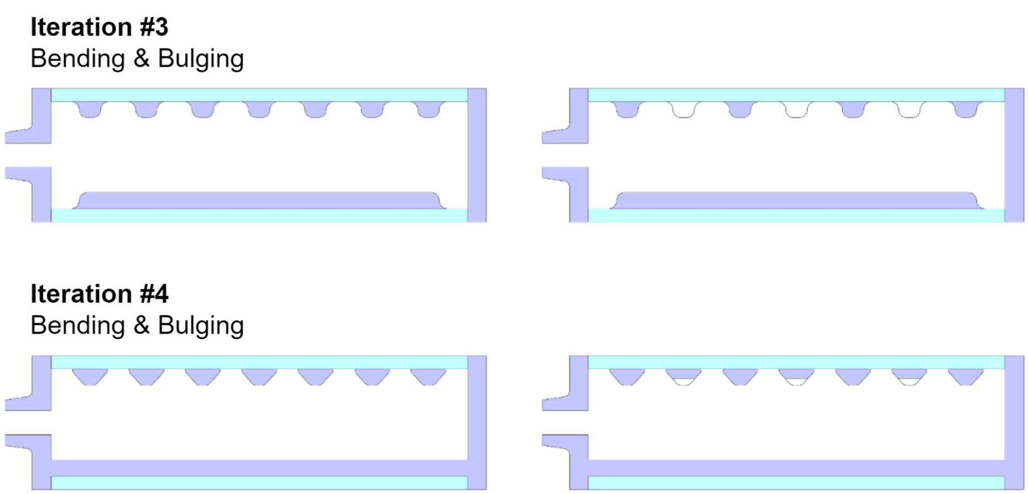


**Figure 9.** Actuator Strain Limiter Profile - Fourth Iteration

# CHAPTER 4

# MATERIAL AND FABRICATION

## *Introduction*

To examine the actuator designs, a series of modular 3d-printed mold sets for silicone casting was designed for each iteration. Since all actuator iterations feature enclosed envelope designs with only one air inlet and different internal structures, every set of molds was designed based on the idea of partial casting and natural lamination between casted pieces and freshly poured silicone. Also, the modular mold design featuring swappable mold core units with various forms was crucial to achieving different actuator internal structures.

## *Materials*

Silicone rubber products made by Smooth-on were used for the entire project for accessibility, translucency, and ease of fabrication. Through the design process, the selection of material changed for each iteration due to revisions in structures and compositions, resulting in different mechanical properties requirements **(Figure 10)**.

| | Dragon Skin™ 10 FAST | Dragon Skin™ 20 | Ecoflex™ 00-30 | Ecoflex™ 00-50 |
|---|---|---|---|---|
| *Product Type* | Silicone Rubber - Platinum Cure<br>Flame Rated Materials<br>Skin Safe FX Materials | Silicone Rubber - Platinum Cure<br>Skin Safe FX Materials | Silicone Rubber - Platinum Cure<br>Skin Safe FX Materials | Silicone Rubber - Platinum Cure<br>Skin Safe FX Materials |
| *Mixed Viscosity* | 23,000 cps | 20,000 cps | 3,000 cps | 8,000 cps |
| *Pot Life* | 8 minutes | 25 minutes | 45 minutes | 18 minutes |
| *Cure Time* | 75 minutes | 4 hours | 4 hours | 3 hours |
| *Shore A Hardness* | 10 | 20 | 00-30 | 00-50 |
| *Die B Tear Strength* | 102 pli | 120 pli | 38 pli | 50 pli |
| *Tensile Strength* | 475 psi | 550 psi | 200 psi | 315 psi |
| *Elongation @ Break* | 1,000 % | 620 % | 900 % | 980 % |
| *100% Modulus* | 22 psi | 49 psi | 10 psi | 12 psi |

**Figure 10.** Material Selection

The first iteration used Dragon Skin 10 for all parts of the actuator, and the samples produced were rather stiff. Due to the flat envelope design, the material was not too difficult to work with and was able to perform adequately.

However, when fabricating the first sample during the second iteration, where the design drastically changed from a flat envelope to a square tube with thinner wall thickness, Dragon Skin 10's high viscosity made it incredibly difficult to fill tiny corners and tricky undercuts. As a result, it was replaced by Ecoflex 00-30, which has the smallest viscosity and 100% modulus. Since the transformation of an actuator is solely based on differentiating its surface expansion at various locations, which is generated by the placement of "strain limiters" - thickened reinforcement attached to the inner sidewall of the actuator, making these strain limiters significantly stiffer than unreinforced areas is critical. During the second iteration, it was found that Ecoflex

00-30 was overly flexible, largely reducing the effect of strain limiters within the actuator.

As a result, a duo-material approach was adopted in the third iteration. Ecoflex 00-50, which is slightly stiffer than Ecoflex 00-30 but is far less prone to tearing when under pressure, was used for the sidewall part of an actuator. Dragon Skin 10, which is much stiffer than any Ecoflex product, was used for all strain limiters. This approach yielded quite positive results, raising the maximal allowable pressure from 2 psi to 7 psi. This was made possible because all Dragon Skin and Ecoflex products were platinum cured silicone rubber, allowing them to laminate to each other naturally. However, Dragon Skin 10 was still not strong enough as the middle portion of the actuator would expand much more than sections closer to both ends, giving it a “bloated” look. In this case, Dragon Skin 20 was tested against Dragon Skin 10 using the same actuator structure. The sample unit with strain limiters made of Dragon Skin 20 exhibits significantly better coherency in surface expansion throughout the actuator’s length **(Figure 11)**.


**Figure 11.** Strain Measurement - DS10 vs. DS20

Initially, the suspended membrane was fabricated using Ecoflex 00-50, the same material used for the actuator sidewall. However, several testing samples indicated that the membrane was too stiff and exerted too much stress on the actuator when being stretched. Ecoflex 00-30 was used in later prototypes to solve this problem. Combining the reduced material stiffness and a diminutive thickness of 1mm, new membrane samples can be easily stretched without affecting the position of actuators.

### *Actuator Mold Design and Fabrication*

In the first iteration, two types of mold sets with variations were designed for the samples featuring flat envelope profile (“diaphragm”) and pyramidal envelope profile (“Corner”), each of which represented part of a speculated larger envelope structure. The mold set for the flat envelope type of actuators contains two pieces, with one used to cast the top half where all the structures are formed, and the other used to cast the thicker bottom where the air inlet is shaped. Following the same two-step-process concept, the mold set for the pyramidal type of actuators features similar designs except that it requires some additional assembling work for the top piece to reduce complexity in 3d-printing the mold **(Figure 12)**.

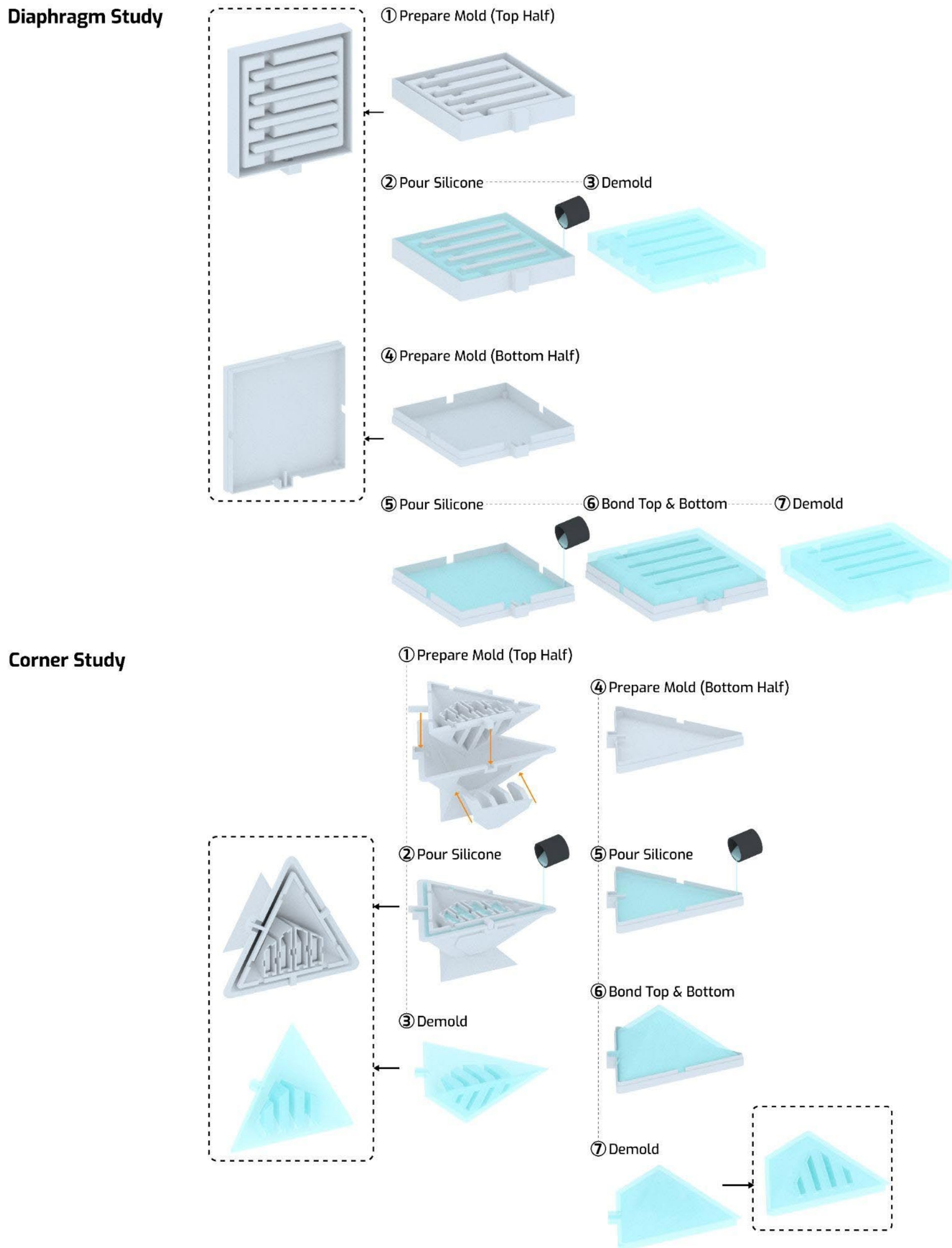


**Figure 12.** Mold Design Concept - First Iteration

Using the corner mold set as an example, once the top mold is assembled, silicone is poured along the edges of the mold. After curing, the top piece is demolded and prepared for lamination. Then, silicone is poured into the bottom mold, and the top piece is immediately placed on top of the uncured silicone to enable lamination. When the envelope is completely cured, it can be removed from the mold for testing **(Figure 13)**. All variations of mold designs used during this iteration of the study are demonstrated below **(Figure 14)**.

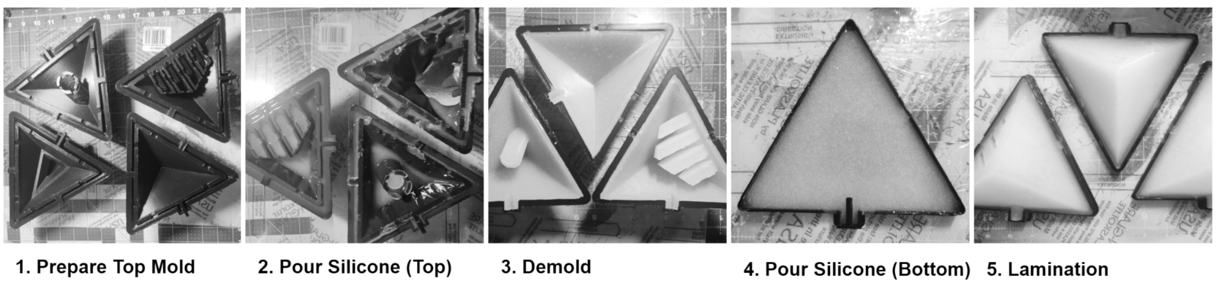


**Figure 13.** Fabrication Process - First Iteration

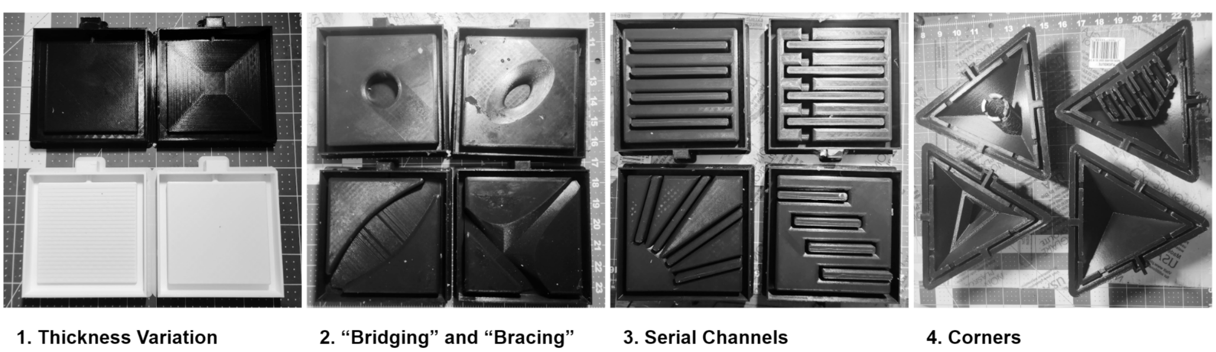


**Figure 14.** Mold Design Variations - First Iteration

Due to the drastic change in actuator design strategy, the mold used for the second iteration of the study also featured major design revisions. Due to the new square tube profile, the internal structure of an actuator is now formed by a swappable core unit. The core would then be installed into a mold frame with a removable bottom for ease of demolding. The silicone would be poured into the assembly to cast the sidewall and the flat bottom of the actuator, and once cured, the open-ended envelope would be placed vertically into another mold piece filled with a layer of fresh silicone for capping. To prove the feasibility of this mold design strategy, a half-size actuator sample was fabricated **(Figure 15)**.

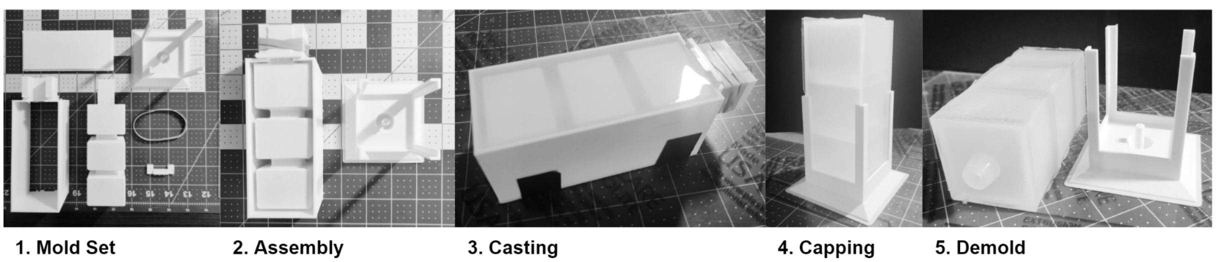


**Figure 15.** Preliminary Mold Design and Fabrication Process - Second Iteration

Based on the positive result, this design was adopted for sample production of full-size actuators **(Figure 16)**. However, the cantilevered connection between the core unit and the mold frame started to exhibit issues as the weight of the core unit increased for full-size actuators. The unsupported end of the core unit would sink slightly below the supported end, resulting in the actuator’s unequal sidewall thickness, hence the unexpected bending behavior in testing. Also, the removable bottom piece was initially attached to the frame mold using duct tape, which was inadequate in maintaining a tight seal, causing massive silicone leakage. Despite the later use of braces, this design could not meet the fabrication requirement.

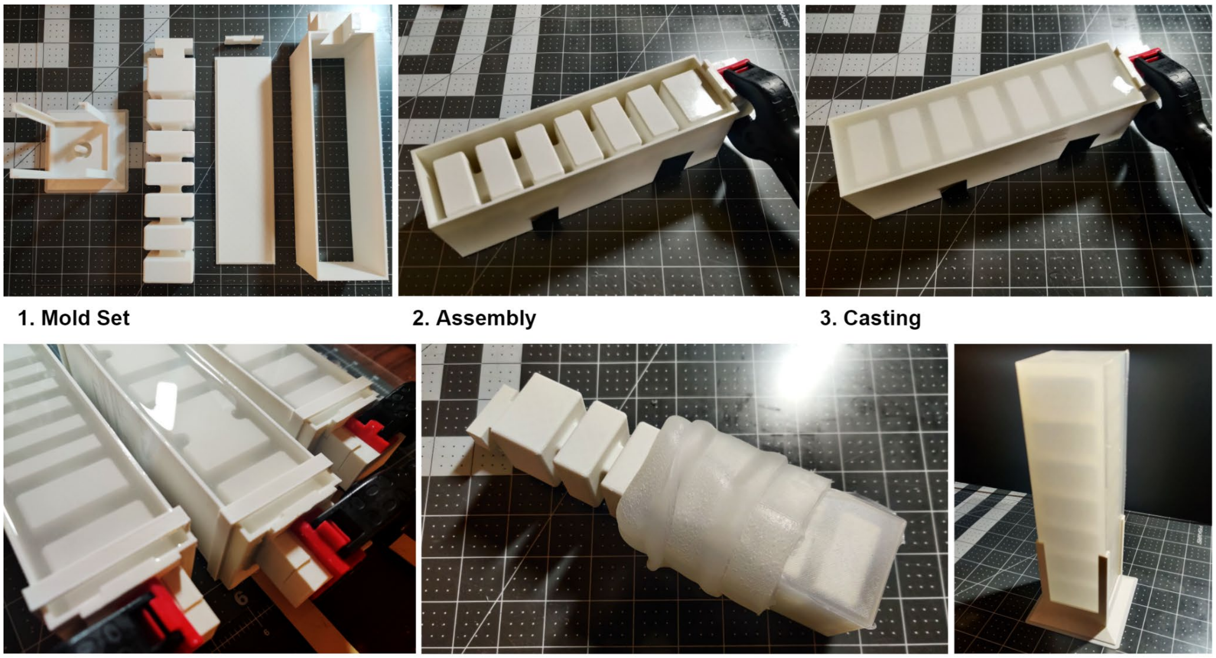

1. Mold Set 2. Assembly 3. Casting

4. Braces 5. Remove Core Unit 6. Capping

**Figure 16.** Final Mold Design and Fabrication Process - Second Iteration

To solve the problems mentioned above in the second iteration of mold design and accommodate the dual-material design approach of the third iteration, several major revisions were made to the updated mold design. First of all, the swappable core unit is supported on both ends to ensure consistent leveling during fabrication. This came at the cost of an additional step of capping after the sidewall was cast. Secondly, one additional set of mold frames with smaller dimensions was introduced into the system for casting the strain limiters. Third, all mold pieces are now connected using clamps to prevent silicone leakage. Six evenly placed tabs located at the bottom of the mold frame and a groove on the bottom plate were implemented to ensure a good seal through the fabrication process. Moreover, edge chamfers and pull tabs are also added to the design to reduce the effort needed in demolding **(Figure 17)**.

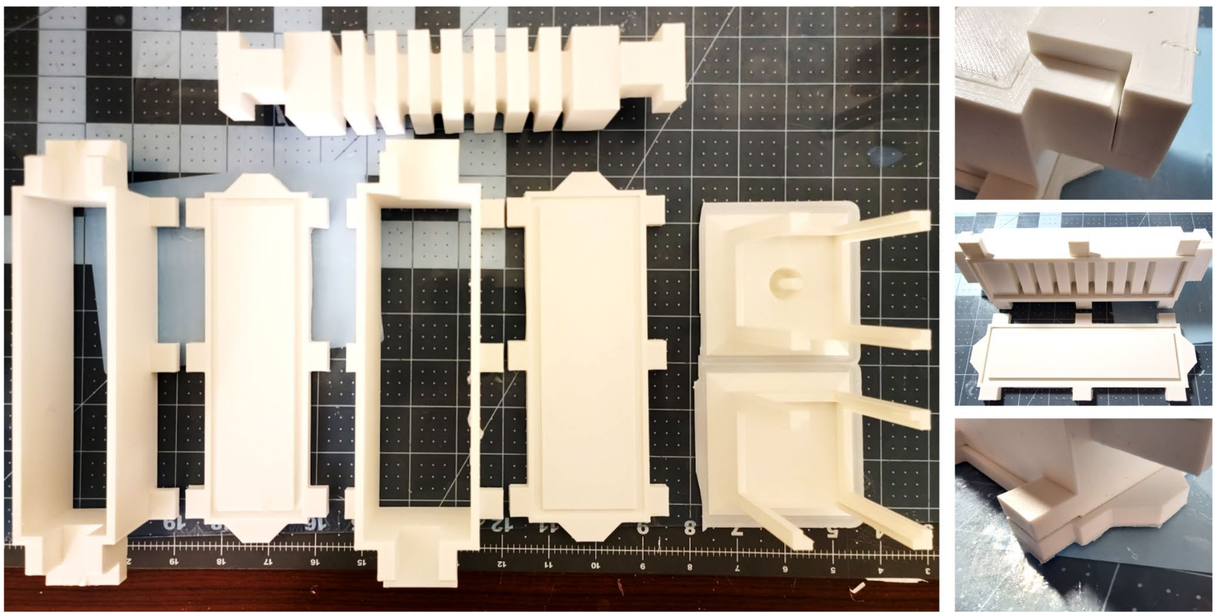

**Figure 17.** Mold Design - Third Iteration

Using this mold design, a four-step-casting fabrication process is required. First, the core unit is attached to the smaller mold frame, and silicone is poured into the assembly to cast the strain limiters using Dragon Skin 20. After curing, the silicone, along with the core unit staying in place, is demolded from the smaller frame, and installed to the larger frame to cast the sidewall. Then, the finished piece is demolded, and the core unit is removed. The open-ended actuator is vertically placed in the third mold for top casting and then the fourth mold for the bottom casting **(Figure 18)**.

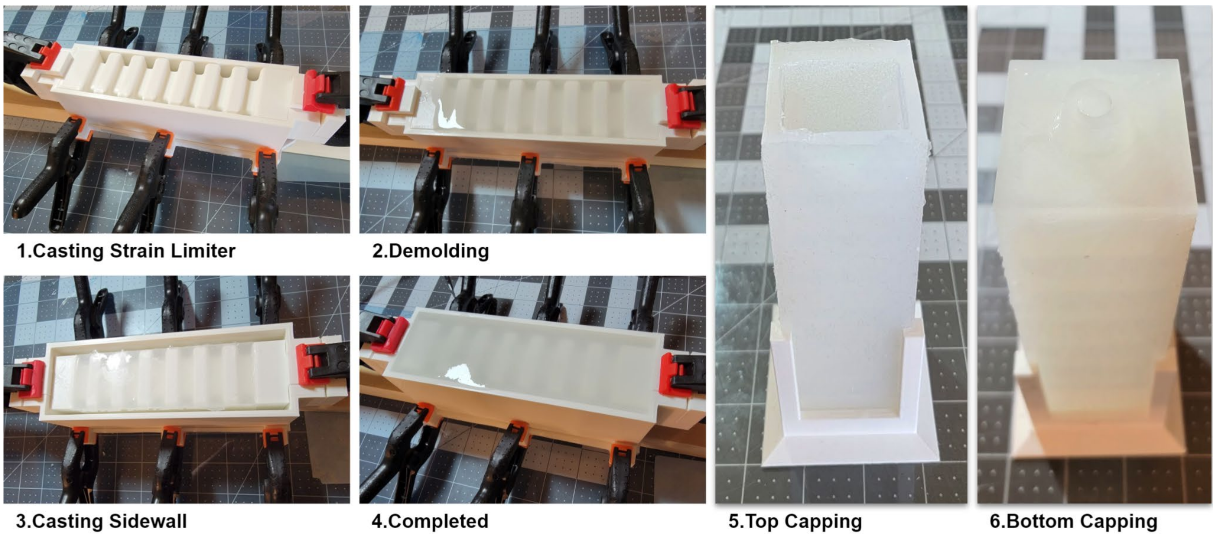


**Figure 18.** Fabrication Process - Third Iteration

These revisions caused a significant improvement in production consistency. However, demolding from the two sets of mold frames was difficult. As a result, the fourth iteration of the mold design added a slot where a lever bar could be inserted to lift the end of the core unit. In addition, the core unit design was modified to accommodate the updated strain limiter profiles **(Figure 19)**. These final revisions have made the fabrication process relatively effortless.

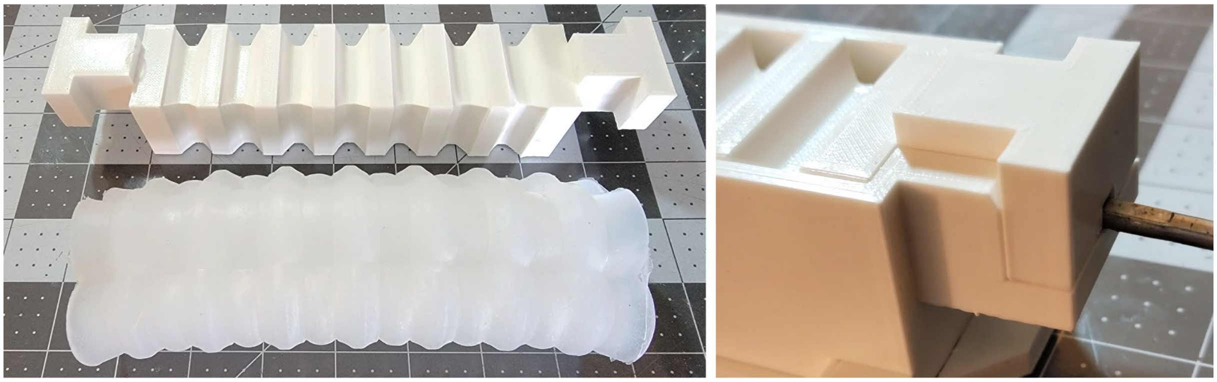

1.Revised Strain Limiter Profile 2.Slot for Lever

**Figure 19.** Mold Design Revision - Fourth Iteration

### *Membrane Mold Design and Fabrication*

The concept of the actuator-membrane assembly was adopted during the second actuator design iteration. The initial iteration of the membrane fabrication process utilized two brackets to hold both actuators on a piece of acrylic panel, and silicone was poured onto the area enclosed within **(Figure 20)**.

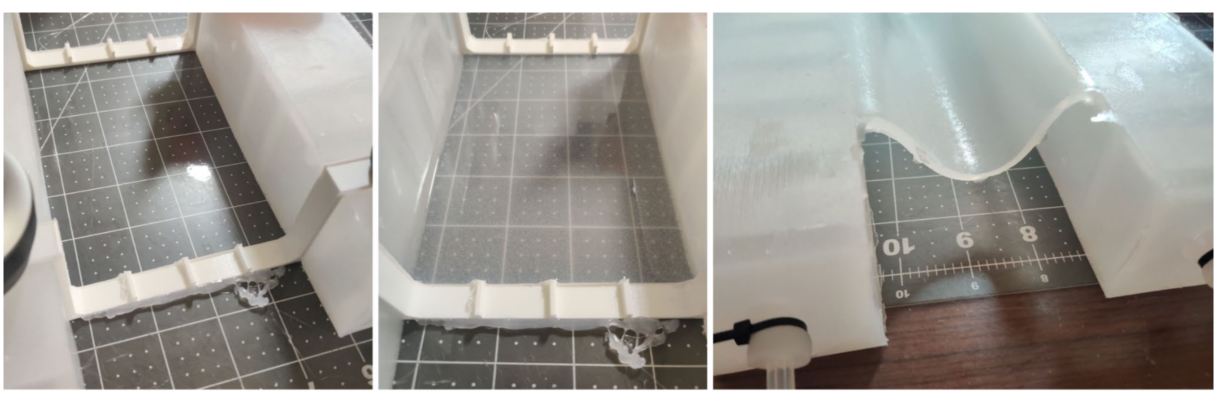

1.Install Brackets 2.Pour Silicone 2.Demold

**Figure 20.** Membrane Fabrication - First Iteration

However, it was difficult to achieve good sealing around the bracket, and several weights and hot glue were required to complete the testing sample. Considering the challenge of casting membrane directly onto the actuator and potential limitations in scalability, a concept for a detachable membrane using magnets and iron powder infused silicone membrane was drafted and tested. Immediately after the strain limiters are cast, two arrays of small magnets are glued directly onto them using Sil-poxy (Smooth-on). Then the casting of the actuator sidewall would then serve as a layer of over-molding that secures those magnets in place. In the meantime, iron-powder-infused silicone strips were produced and then bonded to the rest of the membrane. Although the attachment between the membrane and magnets seemed adequate at lower pressure, the rapid actuator surface expansion under higher pressure easily set them apart **(Figure 21)**.

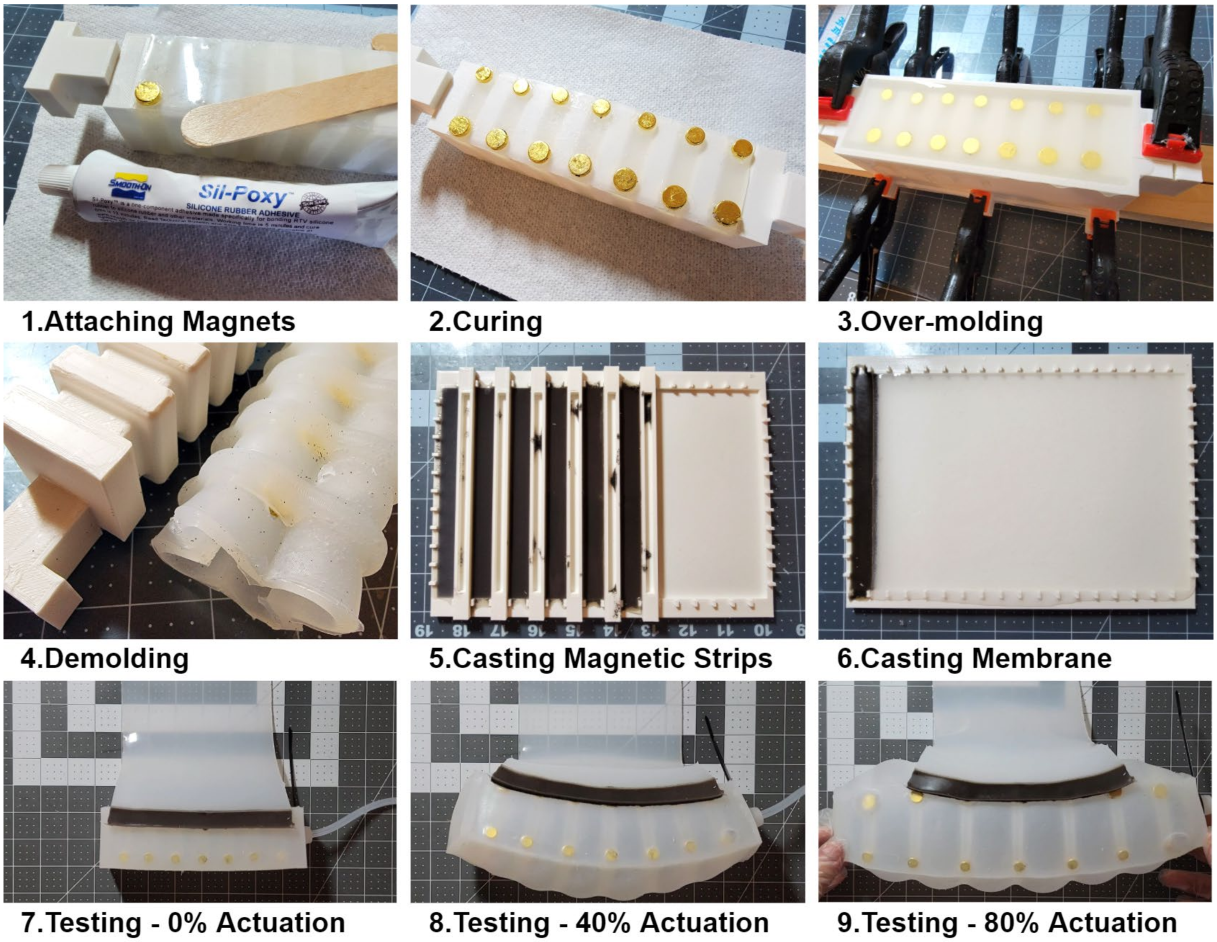


**Figure 21.** Membrane Design and Fabrication - Second Iteration

With a good understanding of the challenges from this detachable membrane design, the direct-cast-on method was resurrected for revision. In the third iteration, a modular mold replaced the previously used acrylic panel and brackets to avoid silicone leakage and obtain better control of membrane thickness **(Figure 22)**.


**Figure 22.** Membrane Fabrication - Third Iteration

With this design, several prototypes were produced without major flaws. However, the membrane was found to be too thick that it exerts an excessive amount of stress on the actuators, pulling them away from their positions. To solve this problem, the subsequent iteration of the mold design reduced the sidewall height from 2.4mm to 1.2mm. Also, a two-way connector was added to facilitate assembly using three actuators **(Figure 23)**. During casting, it was found that the table where the mold was situated was not completely level, causing more silicone to flow towards the bottom of the mold, resulting in the membrane's bottom portion being thicker (measured ~2mm) than its top portion (measured ~1mm). This "issue" was turned into an advantage since most of the stretching happens at the top portion. The self-leveling behavior of silicone combined with pouring from the top allows less material to be used while maintaining even coverage.

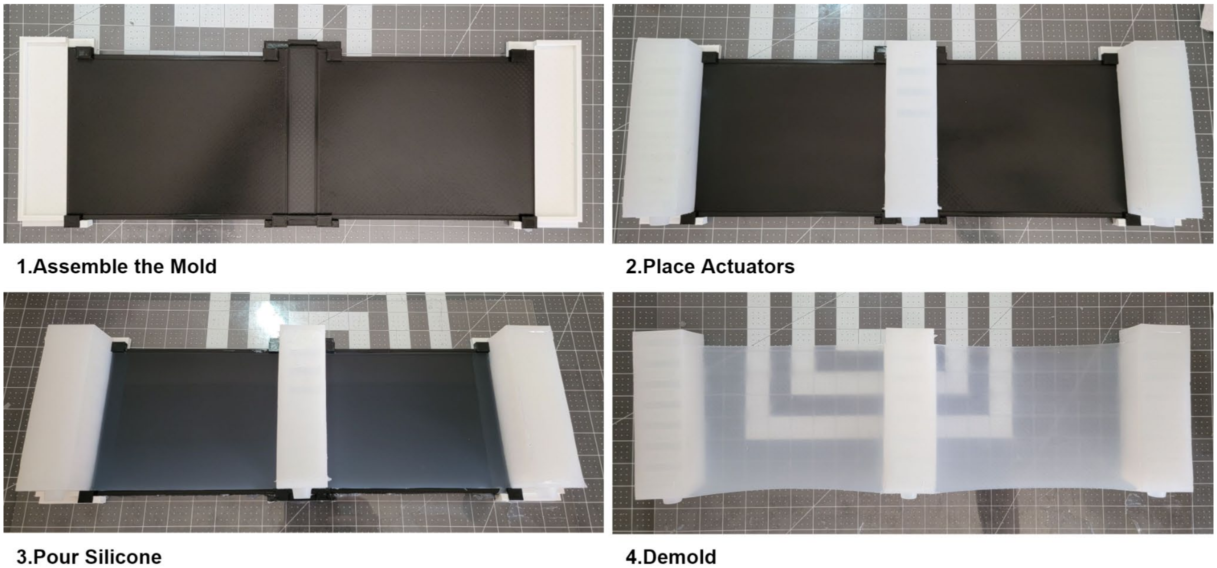


**Figure 23.** Membrane Fabrication - Fourth Iteration

### *Attachment Mechanism Design*

Since the device is designed for shading and partitioning functions, it must be held in place firmly to avoid undesired movements impairing its performance. Inherited from the unsuccessful detachable membrane concept, a magnetic connector was designed to enable quick and easy attachment or reconfiguration while aligning all tubing to the same direction **(Figure 24)**. During testing, it was found that the four small magnets on each connector barely kept the actuators in place but were not able to resist the stress exerted by the membrane when being stretched.

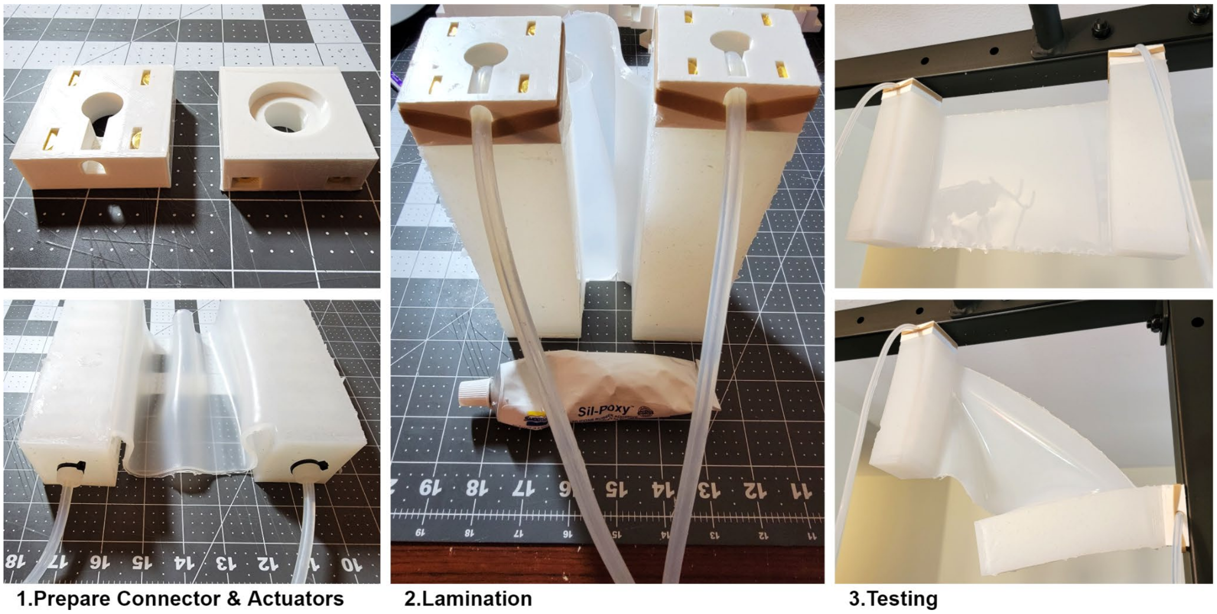


**Figure 24.** Attachment Mechanism Design - First Iteration

To solve this problem, the new version replaced those four small magnets with two 5mm thick bar magnets and added two sets of anchors, which could be connected using link bars to maintain the relative position of the two actuators **(Figure 25)**.

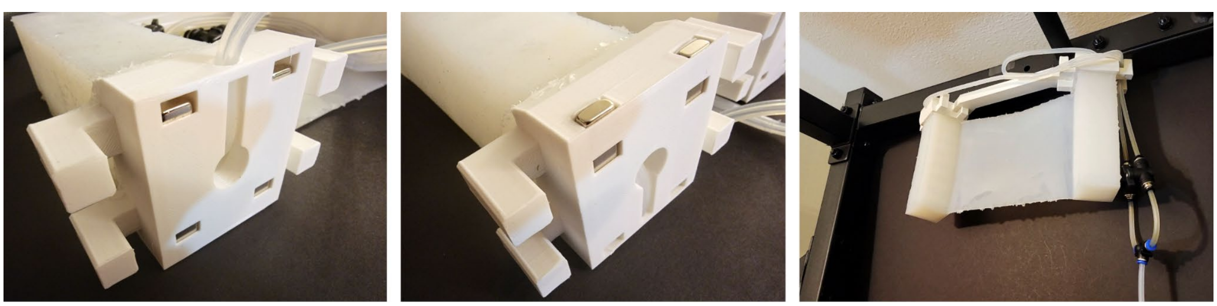

**Figure 25.** Attachment Mechanism Design - Second Iteration

The new design performed adequately during testing, and the pulling force from the two bar magnets was strong enough even for outdoor situations. During the fourth iteration of the actuator design, a minor revision of the connector was made to accommodate changes from using ¼'' OD tubings to ⅜'' OD tubings **(Figure 26)**.

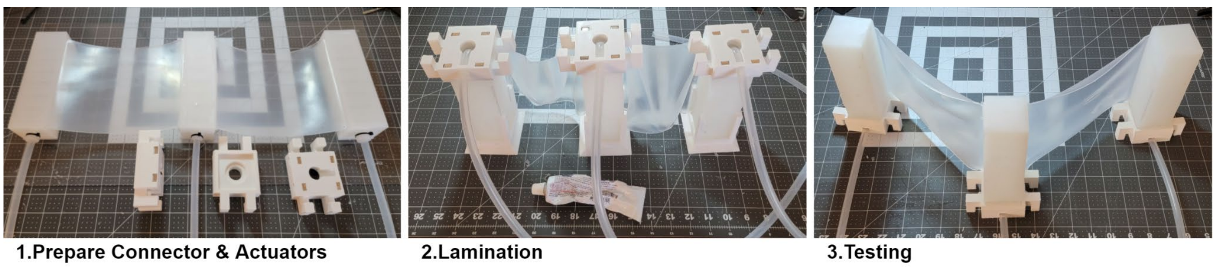


**Figure 26.** Attachment Mechanism Design Revision - Third Iteration

# CHAPTER 5

# DIGITAL SIMULATION

### *Introduction*

Considering the relatively demanding fabrication process and high cost of materials, digital simulation in Grasshopper, a parametric design interface integrated with Rhinoceros 3D, was used to conduct preliminary design speculations for large-scale installations based on the actuator-membrane device developed in previous chapters. The simulation's sole purpose was to provide a visual reference for interaction design; no physical simulation that predicts and examines individual components' material and structure was involved in this stage. Instead, measurements of sample actuator units before and after air inflation were applied in the calibration process of the digital reconstruction program to maintain an acceptable level of fidelity. Once the actuator reconstruction program was completed, it was embedded into an aggregation program to simulate the desired scale of the installation. Spatial parameters such as shifting in the x,y,z directions and rotating according to the x,y,z axis were used to fine-tune the aggregation composition and provide a basic structure for several modes of interaction according to external conditions. The complete Grasshopper program is included in the Appendix section.

***Actuator Digital Reconstruction***

The digital reconstruction process of each actuator unit is divided into three steps: cross-section profile building, central axis building, and surface lofting from all curves generated in the two previous steps.

The first step is to create the cross-section profile of the actuator. Through the length of an inflated actuator, it is evident that surface expansion conditions differ at three locations: caps (top & bottom), strain limiter, and middle of each section. Therefore, the respective expansion ratio of each section profile was set to different values on top of the standard expansion ratio based on the level of inflation. In addition, edge corners always exhibited less expansion than the edge centers due to the square section profile that all actuator units featured. As a result, an additional expansion factor was applied to the edge center. Moreover, some actuator units feature solid backing on one side, which would result in significantly restricted strain under pressure. Therefore, expansion factors were also adjusted for these conditions **(Figure 27)**. By manipulating some of these parameters, the exact transformation from 0% to 100% of inflation can be precisely adjusted to match the behavior of the sample unit **(Figure 28)**.

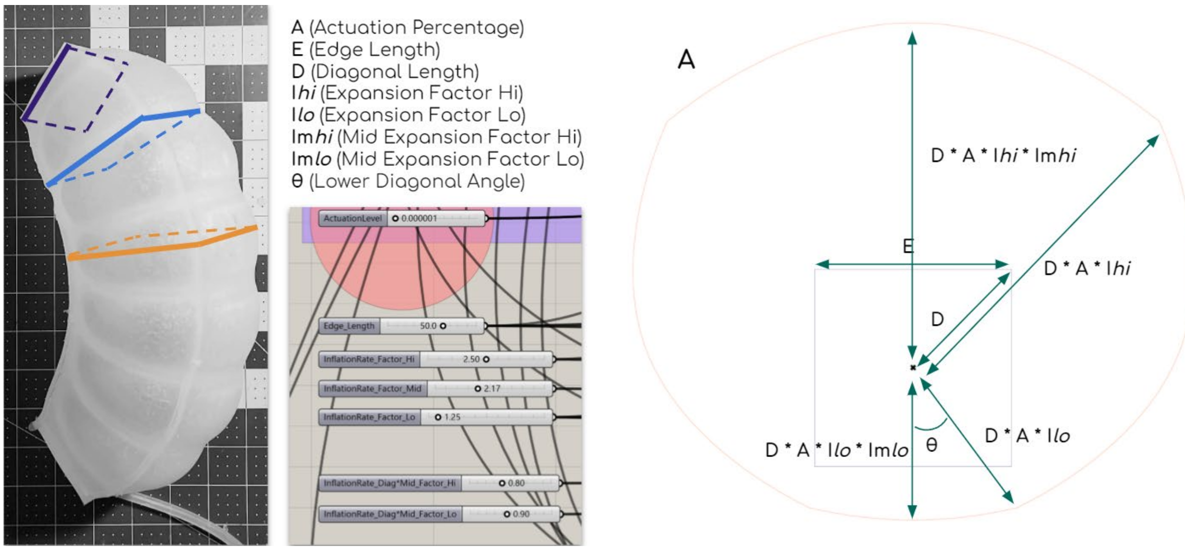


**Figure 27.** Digital Simulation - Actuator Section Profile Construction

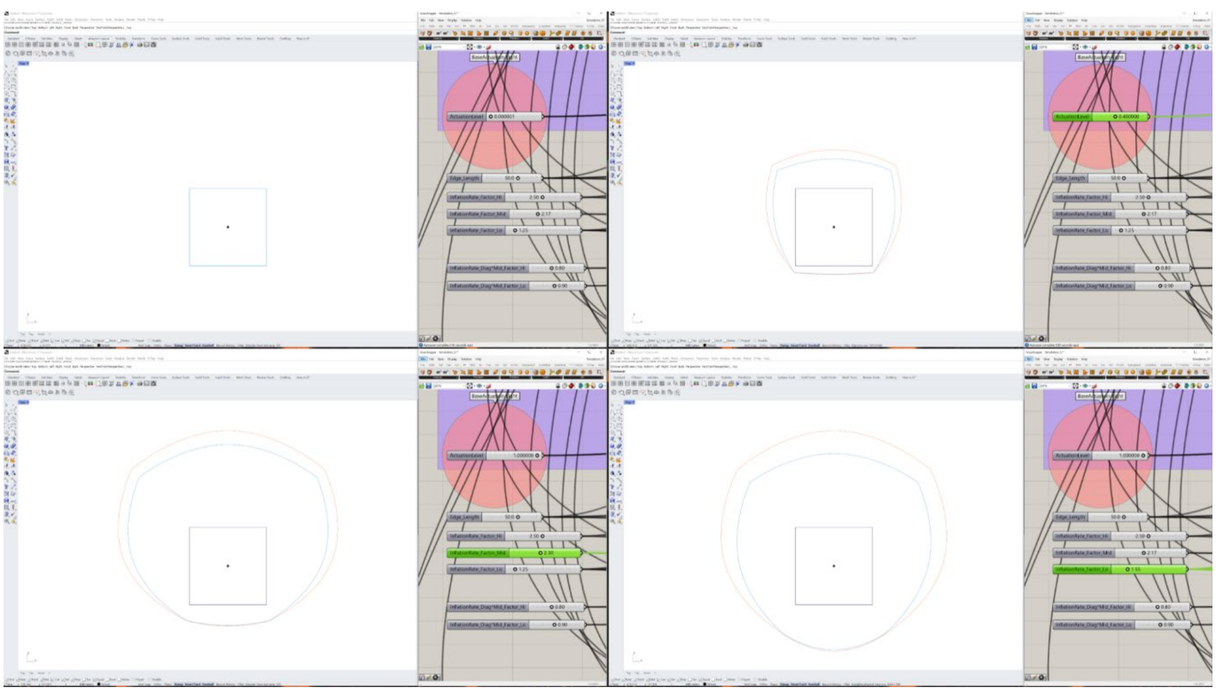

**Figure 28.** Digital Simulation - Actuator Section Adjustment

The second step is to create the longitudinal axis that connects the center of each section profile drawn from the first step. A sample diagram containing the lower half of a section and the upper half of the section right below it was defined to calculate the deformation. Due to the noticeable inconsistency in bending angles among all sections, an approximation process was used to simplify the process so that the bending now only exist at the middle of each section. The axis was turned from a smooth curve into a polyline with this approximation. The two equal quadrilaterals can be defined using trigonometry based on previously defined conditions **(Figure 29)**. Similar to the first step, the exact transformation can be fine-tuned by adjusting the expansion factors **(Figure 30)**.

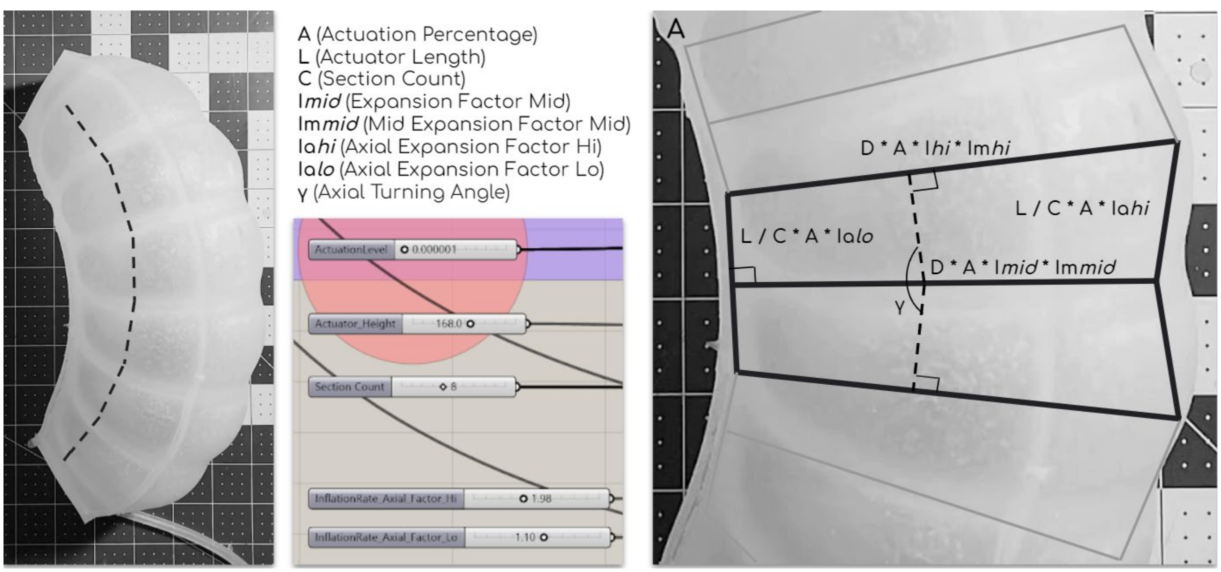


**Figure 29.** Digital Simulation - Actuator Bending Axis Construction

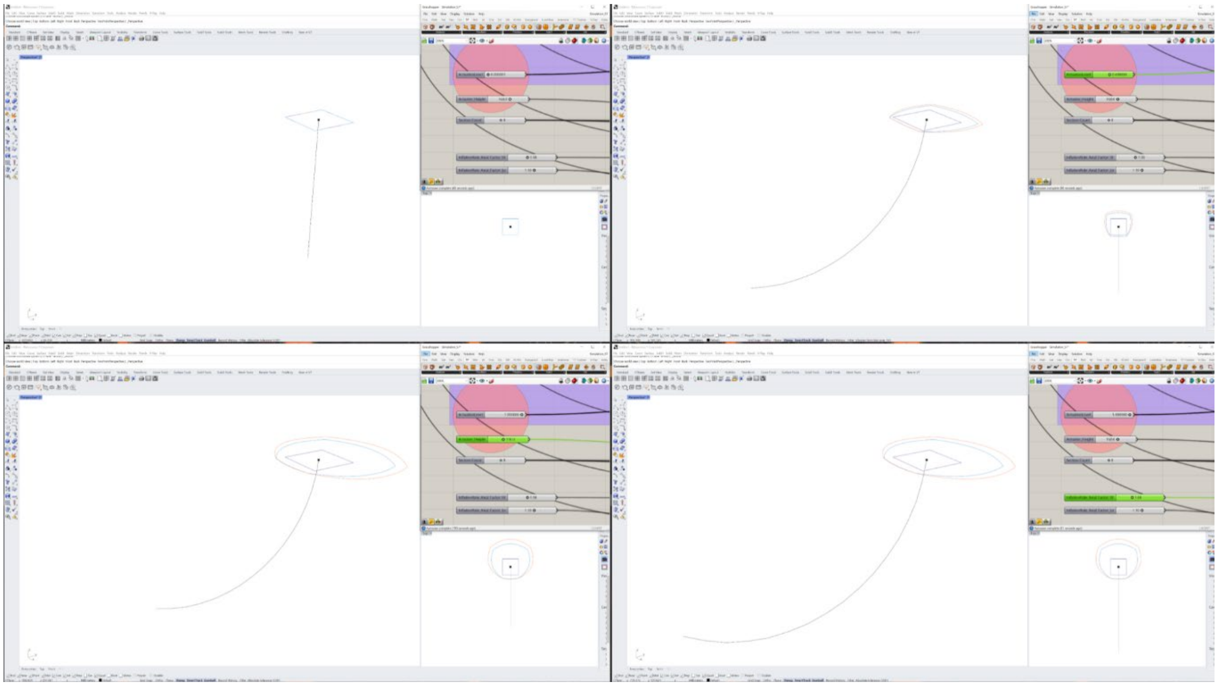

**Figure 30.** Digital Simulation - Actuator Bending Axis Adjustment

Then, the section profiles generated in step one can be duplicated and oriented to their respective position based on their spatial relations to the central axis. Once all curves are in place, a closed surface can be created through lofting. All expansion factors introduced in previous steps can also be used to modify the global shape of the actuator at every inflation stage for calibration purposes **(Figure 31)**.

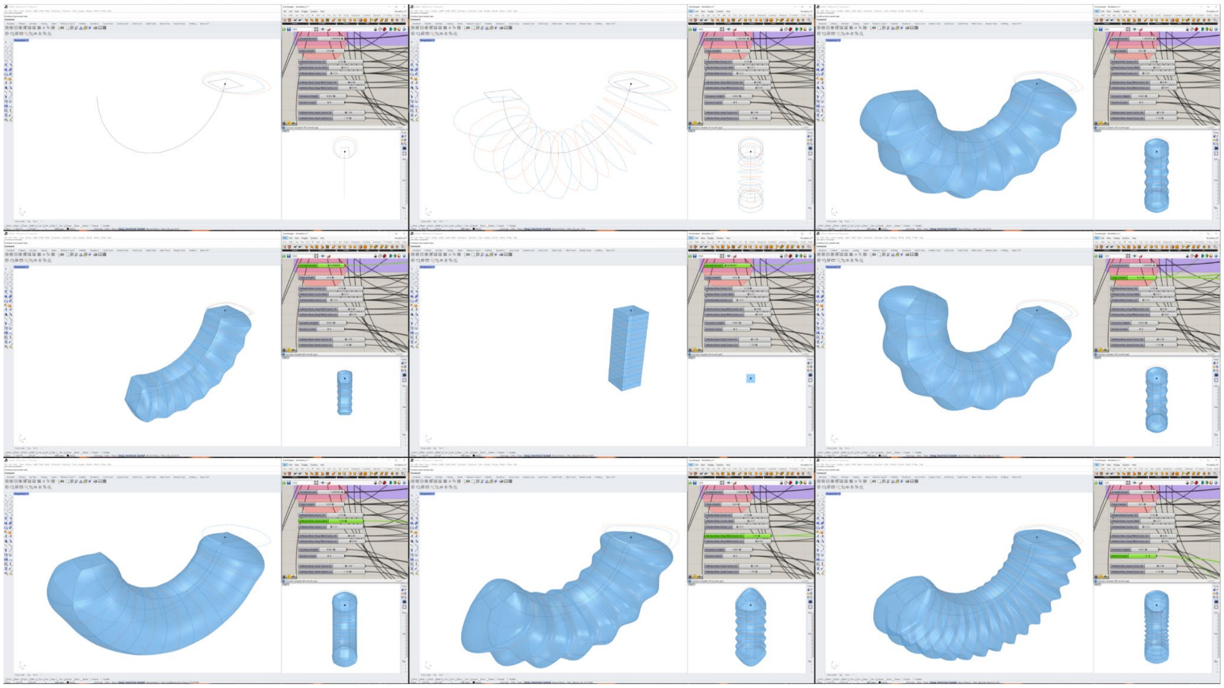

**Figure 31.** Digital Simulation - Actuator Construction and Adjustment

***Aggregation Design***

The potential ways of composition can be studied by aggregating these actuator units into a matrix. When being used as a shading device, the installation's priority in functions and features may differ from when used as a partition device. For example, the former situation would require more flexibility in bending to accommodate various sun angles throughout the day. In contrast, the latter would demand larger surface area coverage or less visibility. By manipulating the spatial attributes of each actuator unit, mainly in the form of shifting and rotation **(Figure 32)**, a set of compositions that feature diverse forms can be generated to achieve optimal results in desired use cases **(Figure 33)**.

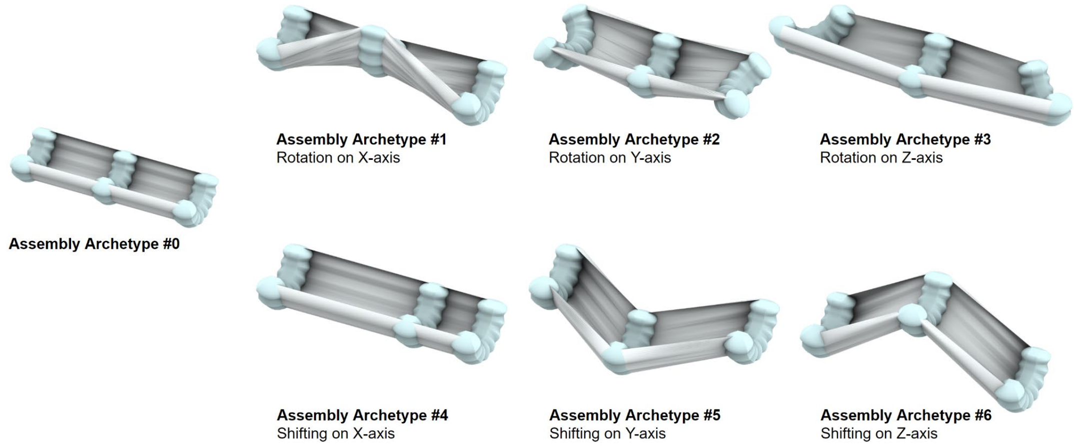


**Figure 32.** Digital Simulation - Actuator Spatial Configuration

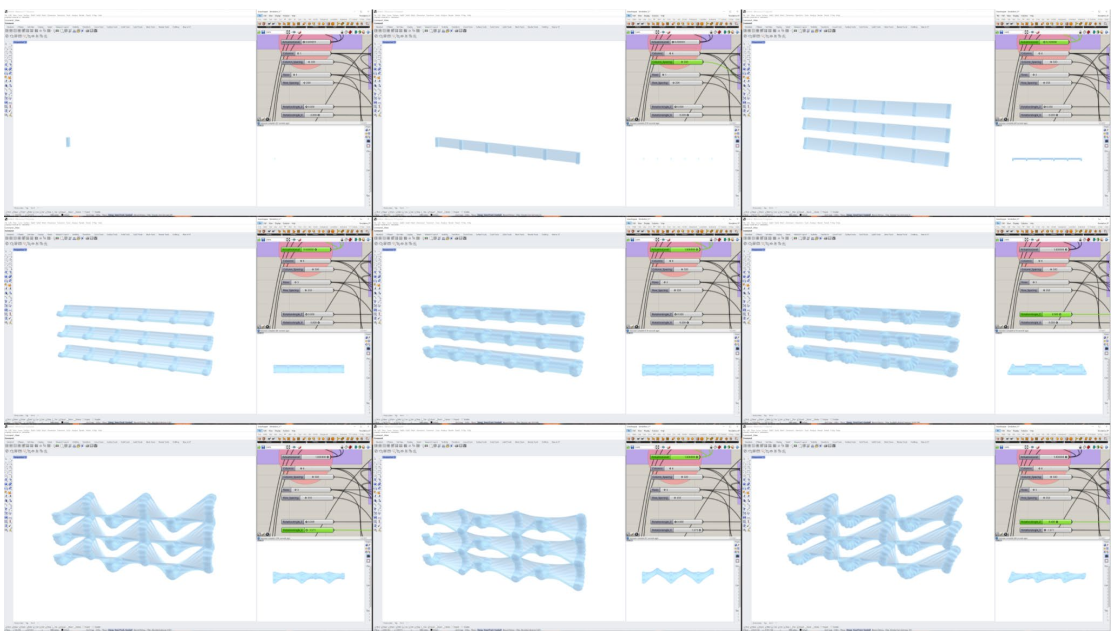

**Figure 33.** Digital Simulation - Actuator Composition Study

### *Interaction Simulation*

Three situations were defined for this preliminary interactive study on how the device would react to external conditions. For clarity purposes, all situations are demonstrated using the basic aggregation formation with all actuator units facing the same direction.

The installation would serve only as a shading device that responds to natural lighting conditions in the first situation. This would require all actuators to synchronize their levels of transformation in order to achieve a coherent shading effect **(Figure 34)**. In some cases, the synchronization could be applied only to actuators within the same row to accommodate height differences in placement.

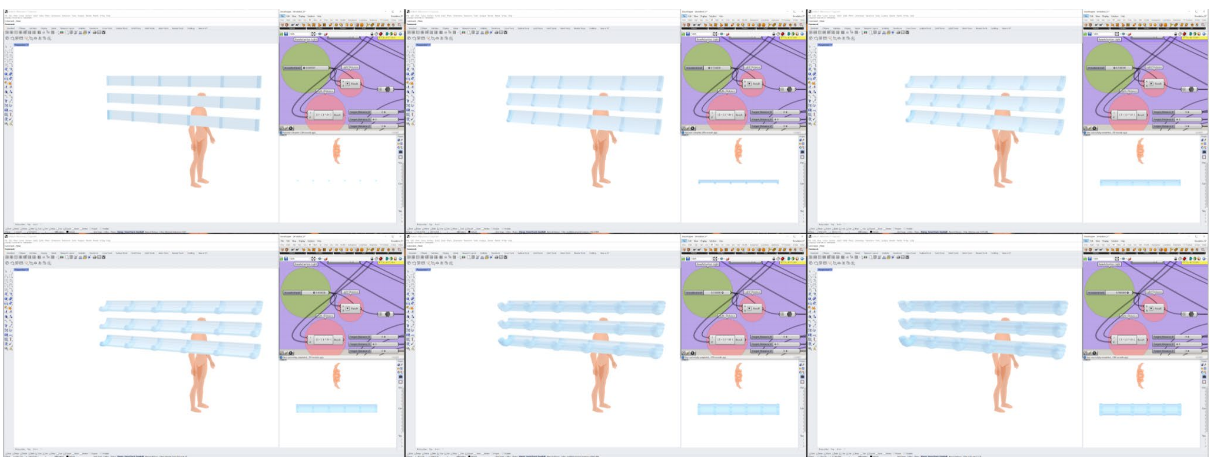

**Figure 34.** Interaction Simulation - Shading

In the second situation, the installation would serve only as a partition device that responds to a human object's distance to help facilitate social distancing in public spaces. Unlike the previous situation, where all actuators work at the same pace, this situation requires differentiation in the inflation level of every individual actuator based on its distance to the target object. Whether the human object is approaching the device or walking alongside the device, each actuator calculates the required pressure and responds spontaneously in real-time. In addition, the actual relationship between distance and actuation level is calculated on a curve to emphasize the effect when the object gets closer **(Figure 35)**.

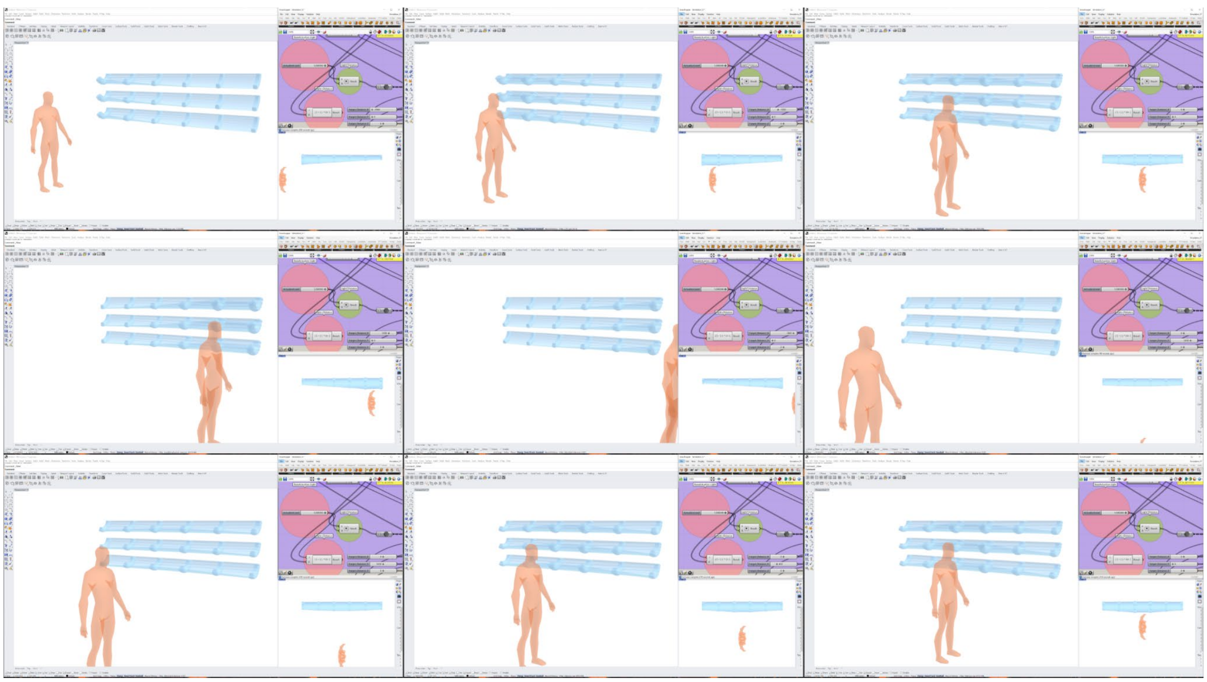

**Figure 35.** Interaction Simulation - Partition

The third situation combines the functions of the two previous situations. The installation works as a shading device but would also respond to close-by moving objects on top of its existing actuation level. In this case, the baseline of actuation is determined by lighting condition, and the actual range of transformation according to distance is between the current level and the predetermined max level of activation, which is constantly changing throughout the day. The correspondence between distance and actuation also needs to be remapped whenever the baseline changes **(Figure 36)**. The series of digital simulations have resulted in a better understanding of the actuator transformation effect, and the preliminary interaction study also contributed to the design of the interactive prototype.

**Figure 36.** Interaction Simulation - Shading + Partition

CHAPTER 6

# INTERACTION AND CONTROL

## *Introduction*

In order to prove the concept raised in the simulation studies, a digital control platform was designed and built to achieve automated interactions with designated external parameters. In addition, three interaction programs were developed and tested to demonstrate their potential functions and impacts. As a functional prototype, the small installation consists of three actuators based on the fourth design iteration and two membranes suspended among them **(Figure 37)**. The outer two actuators are bending units, while the central actuator is a twisting unit. With this configuration, each of the actuators can work independently or simultaneously depending on the program's specific requirements.

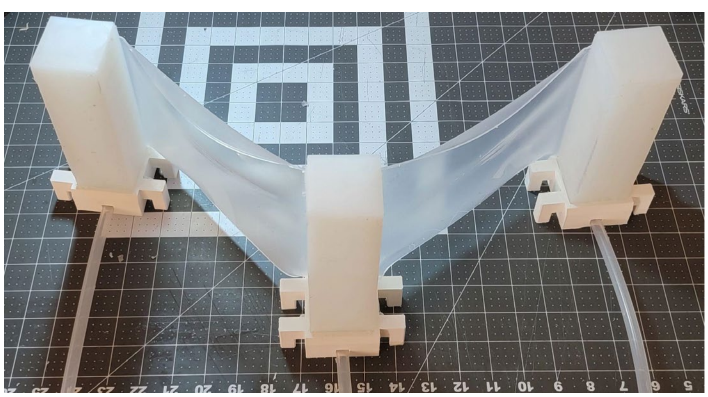

**Figure 37.** Prototype Used for Interaction Study

### *Components and Circuit Design*

Due to the requirement for all actuators to be capable of operating independently, each unit is connected to a dedicated solenoid valve (AOMAG). An additional valve was connected to the main airway for air release. All four valves are attached to a set of splitter manifolds, where a pair of air compressors (Karlsson Robotics) and a pressure transducer sensor (Wal front) are also connected **(Figure 38)**. All components in the airway are connected using silicone tubing with ¼'' Inner diameter, and those that came with ¼'' NPT jacks were adapted to ¼'' barb fitting for the tubing. By coupling two pumps, each rated at 12L/min, the actuation process duration can be significantly reduced, thus accelerating its response to the changing environment. However, this airway design cannot facilitate inflation and deflation simultaneously, which did place some restrictions on the interaction program designs.

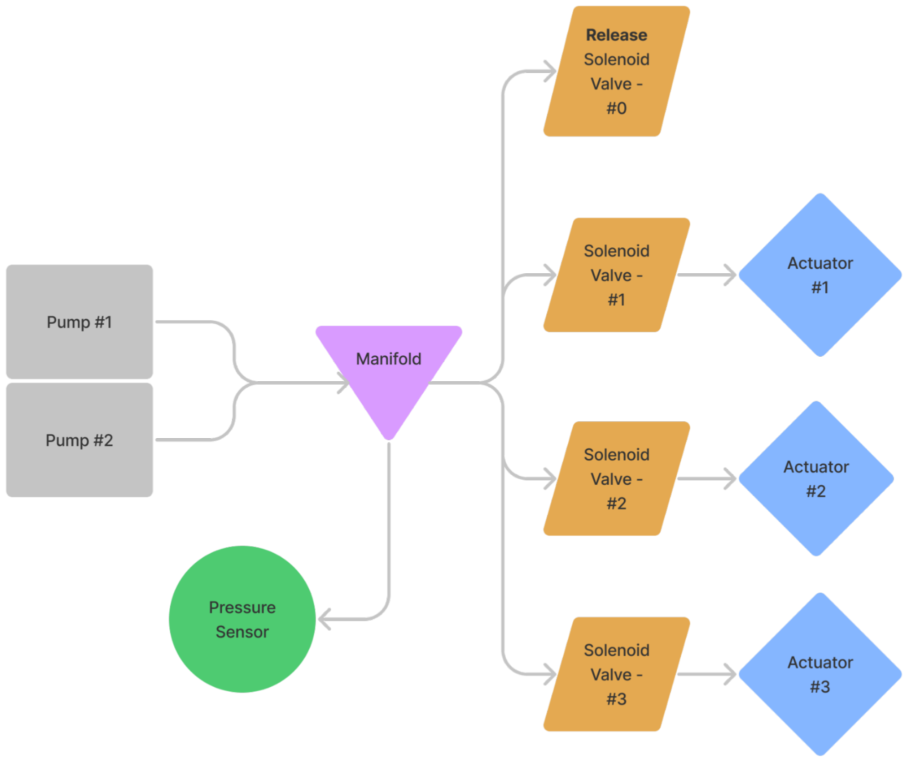


**Figure 38.** Airway Design

A series of motor drivers (L298N) was initially used to control the pumps and valves, but they exhibited inconsistent voltage output to those components during the testing process. Eventually, these motor drivers were replaced by a relay module powered by the 12V power supply and controlled by Arduino directly. The original plan was to place one light intensity sensor (BH1750) on the central actuator and one ultrasonic distance sensor (HC-SR04) on each bending actuator, so the two units could detect their respective distance to a moving object and respond independently. However, due to the previously mentioned limitation from the coupled pumps, one actuator inflates while the other deflating becomes impossible within the current set-up. As a result, only one ultrasonic distance sensor was placed at the center alongside the light intensity sensor, and two outer actuator units are required to be synchronized when this program operates. The circuit diagram **(Figure 39)** and the completed control platform are shown below **(Figure 40)**.

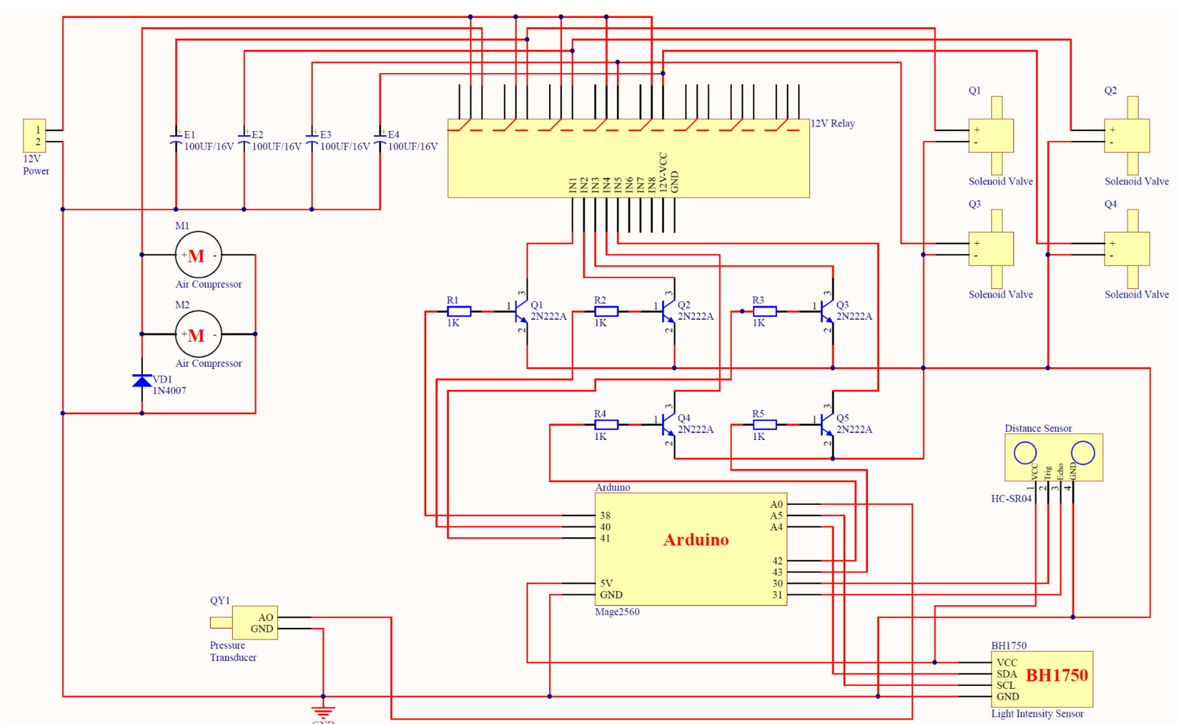


**Figure 39.** Circuit Diagram

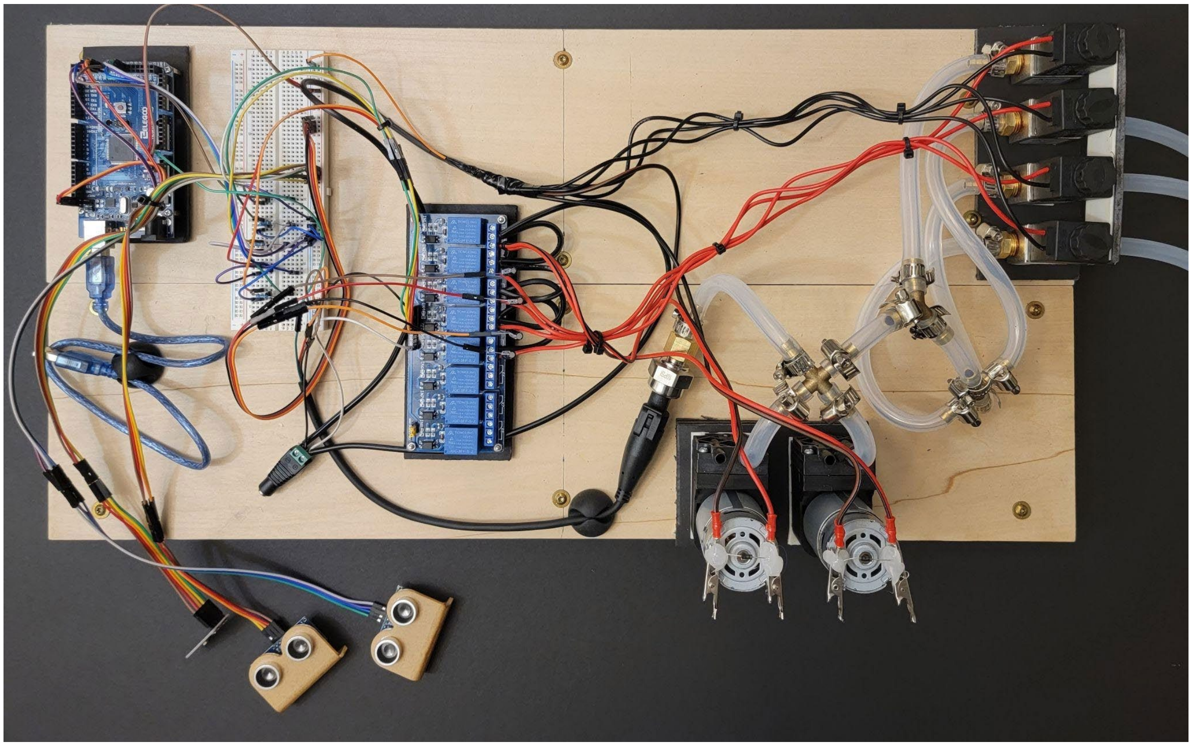

**Figure 40.** Control Platform - Prototype

For modification and testing purposes, the control platform used off-the-shelf components, which are all laid out on a flat test bench. This minimum viable solution does not represent the design intension of a fully integrated system directly attached to each actuator. As part of the speculative study, a design diagram is presented below to demonstrate the ideal form factor and construction of such a system where all components, including the air compressor, the valve, sensors, and the control board are condensed into a single unit that connects an actuator to the frame that provides power **(Figure 41).**

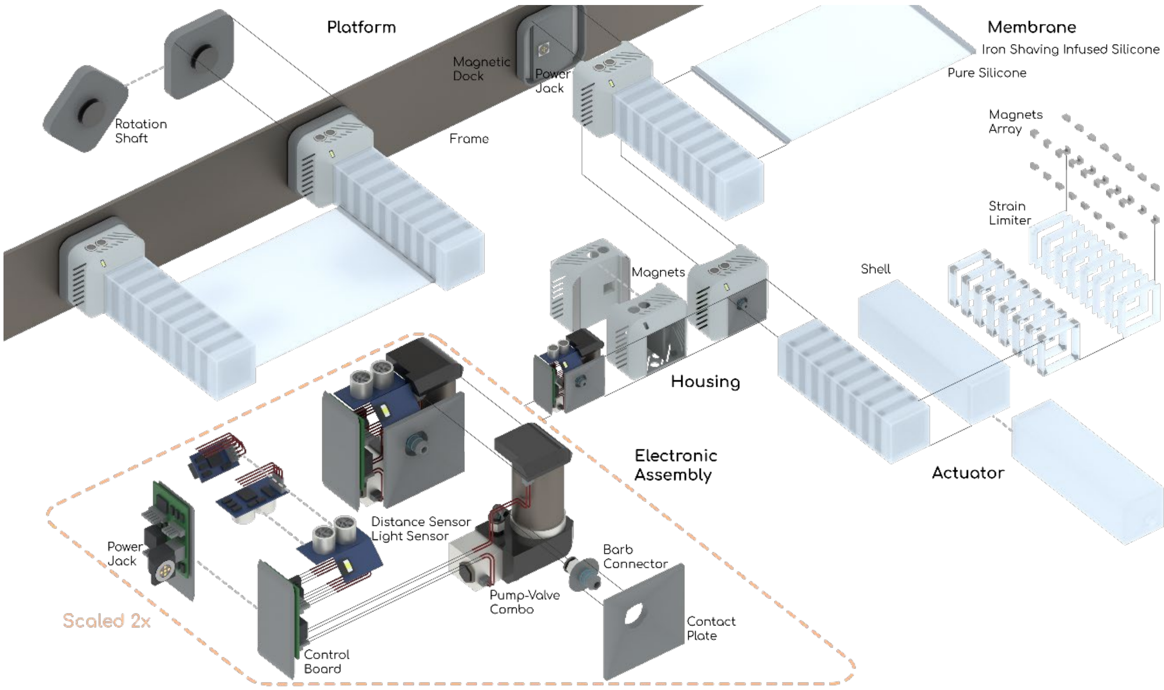


**Figure 41.** Control Platform – Speculative

***Interaction Program***

Evolving from the preliminary interaction studies in the simulation stage, three distinct modes of interaction were identified. In the first mode, the light intensity value is used to calculate the target pressure of active actuators based on a predefined map between the pressure range and the light intensity range. Unlike the first mode, the second mode uses values read from the ultrasonic distance sensor instead of the light sensor to determine the target pressure. The third mode alone does not rely on any external parameters, and actuators activated under this mode would periodically inflate to the max pressure level and then deflate back to their original pressure level to add senses of dynamics to the environment **(Figure 42)**.

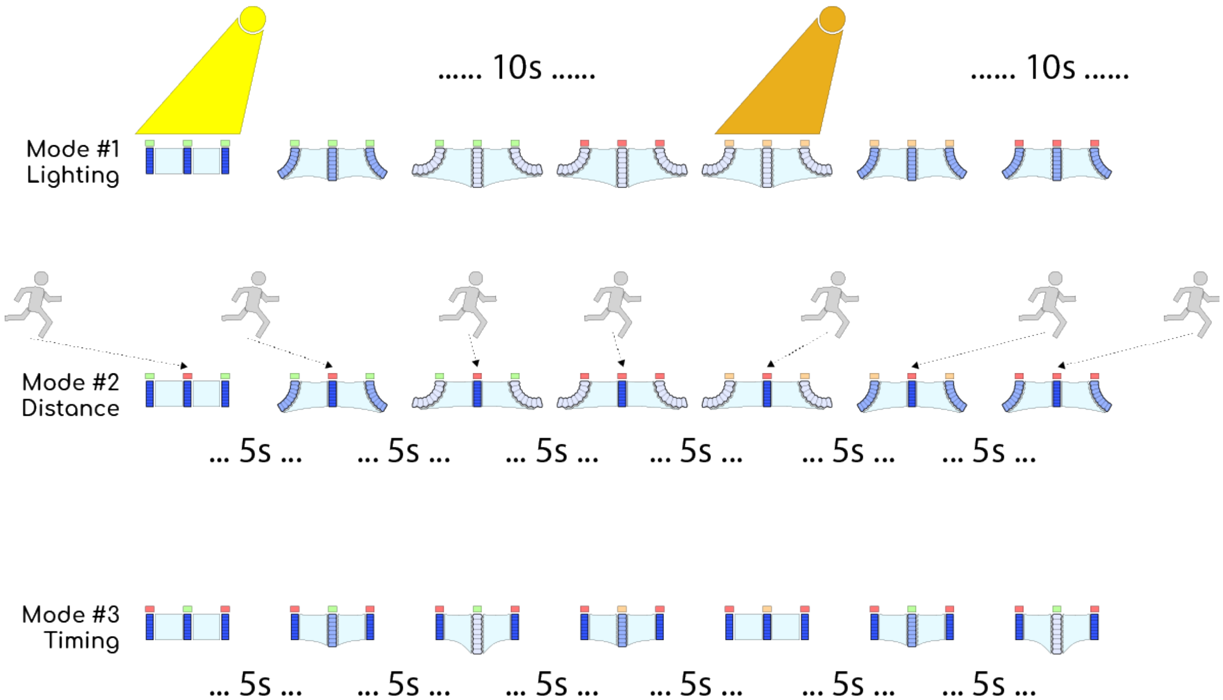


**Figure 42.** Interaction Modes

Three programs were designed for various use cases based on these three modes.

The first program is based on mode one only and serves as a shading device **(Figure 43)**.

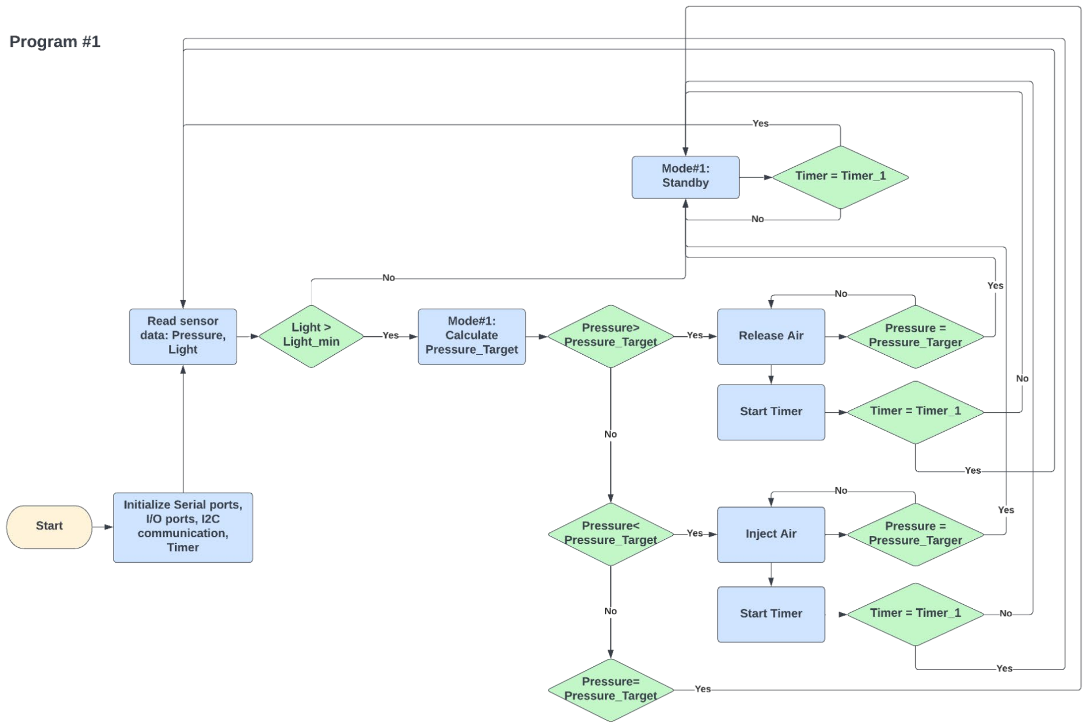


**Figure 43.** Interaction Program #1

The second program is based on the combination of mode one and mode two, with the former prioritized, so it would work as a shading device but could turn into a partition device when needed. The program operates on a set of repeating intervals to make this happen, with the first interval running on mode one and then the rest running on mode two. Also, due to its lower priority, mode two's pressure-distance map in this program is dynamically adjusted using the pressure level determined by mode one from the first interval as the new starting point every time the target pressure is calculated. When program two is executed, all three actuators are activated during mode one, and only the two bending actuators are activated during mode two with the central unit standing by **(Figure 44)**. The third program combines mode one and mode three, following the same logic used in program two. However, only the central unit is activated during mode three. This allows the device to occasionally perform a “show” on top of its shading capabilities to enable a more attractive space **(Figure 45)**.

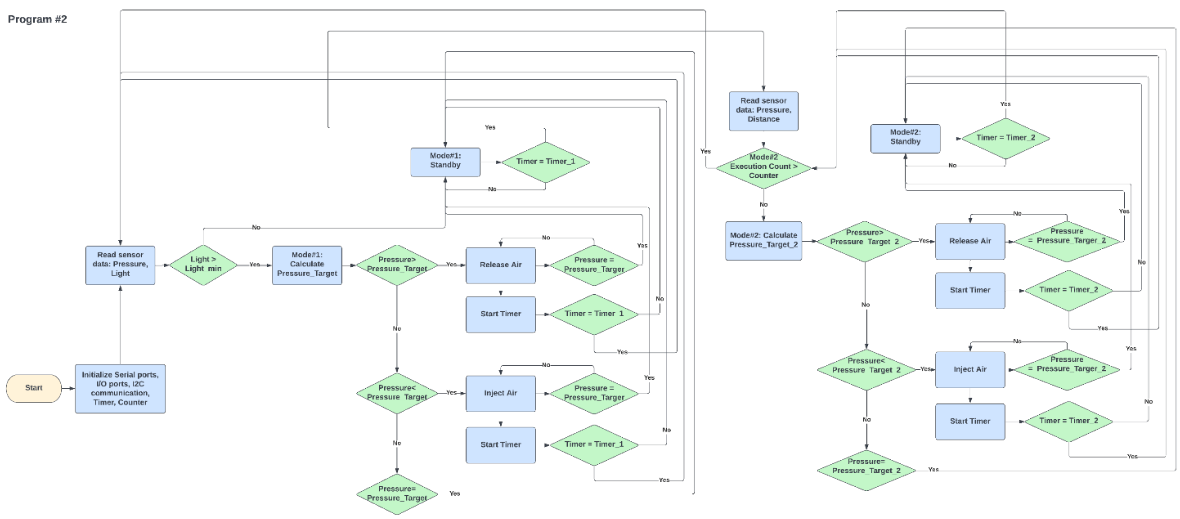


**Figure 44.** Interaction Program #2

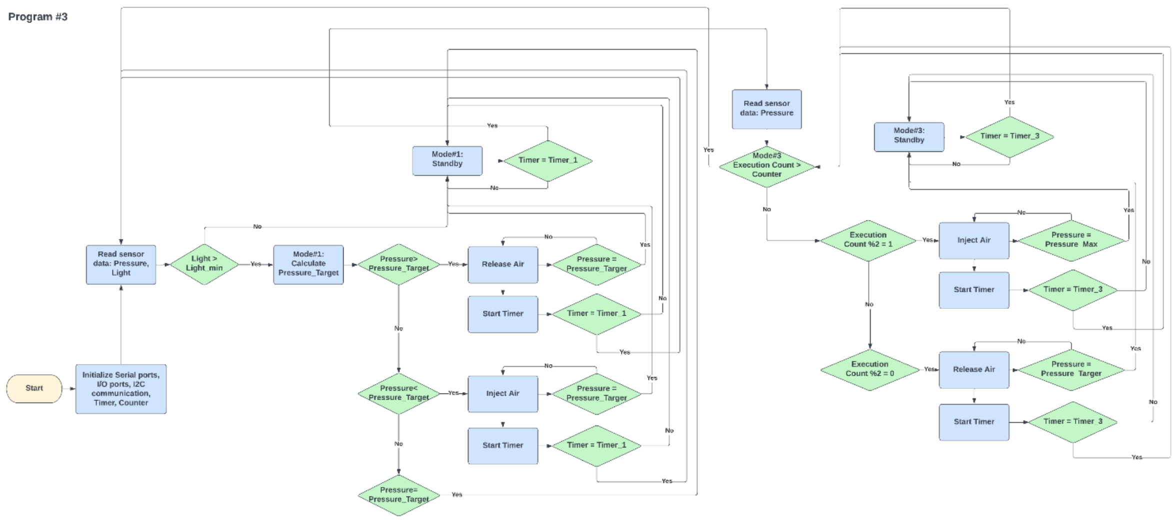


**Figure 45.** Interaction Program #3

Since all the intervals are a standard value arbitrarily determined based on previous observation of the actuation speed, there could be situations where actuators reach target pressure before the interval ends. In this case, the active actuator unit would enter “standby” mode until the next interval starts and target pressure gets updated. In another case, the interval duration might not be sufficient for the actuator to reach the target pressure. To ensure a smooth, coherent reaction, no additional time would be given to compensate for this pressure deficit, and the device would enter the next interval regardless. Sometimes the external parameters remain unchanged, and the device would still execute the routine sensor reading and pressure calculations at the beginning of each interval. However, it would enter “standby” mode and wait for the next interval.

It was discovered during testing that a sudden pressure drop in the sensor reading would occur when inflation stops. Also, during the “standby” session, the pressure would slightly decrease due to potential minimal air leakage. Moreover, since Arduino controls pumps and valves based on action delay intervals (usually set to 100~2000ms), the actuator may get slightly over or under the target pressure level. A set of dynamic compensation values were added to the equation to prevent the device from falsely activating back and forth due to these minor conditions.

To provide a design context for these interactive programs, a set of speculative studies of the device being used for shading are generated. The first situation demonstrates a synchronized transformation across all units in conjunction with the changing lighting conditions throughout the day to accommodate various lighting intensities, sun angles, and desired illumination based on user activities **(Figure 46)**. The second situation presents the local transformation of the device to increase illumination at a designated area where people gather **(Figure 47)**. The third situation exhibits the device’s capability of detecting moving objects and transforming based on the distance **(Figure 48)**. This function allows the shading device to visually signify users to maintain social distancing in public spaces. The third situation illustrates a localized transformation based on time intervals, enabling the device to work as a health habit reminder **(Figure 49)**. These speculative drawings offered an opportunity to examine the device’s integration into the built environment and consider potential design strategies.

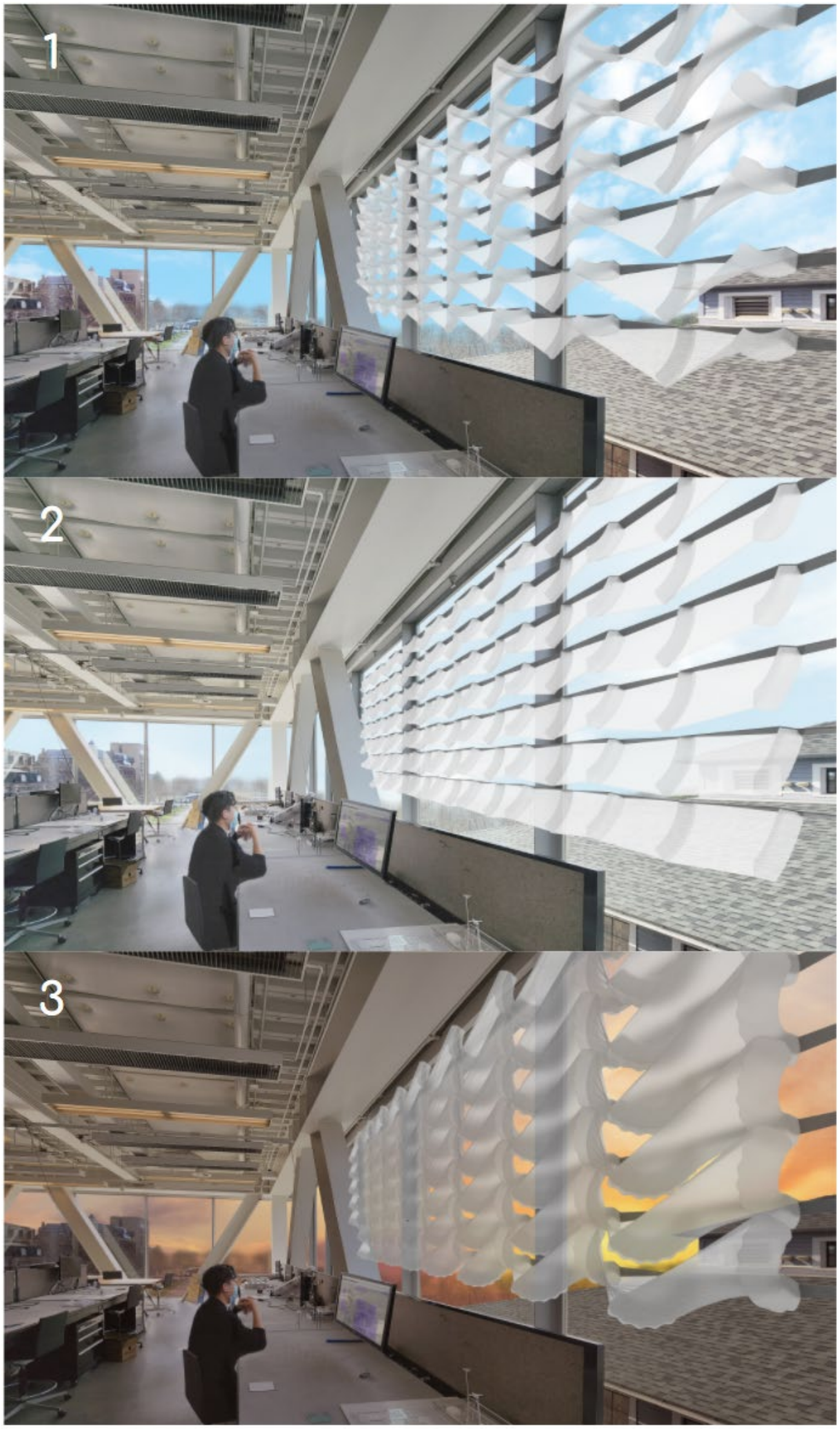


**Figure 46.** Design Speculation – Global Light Conditioning

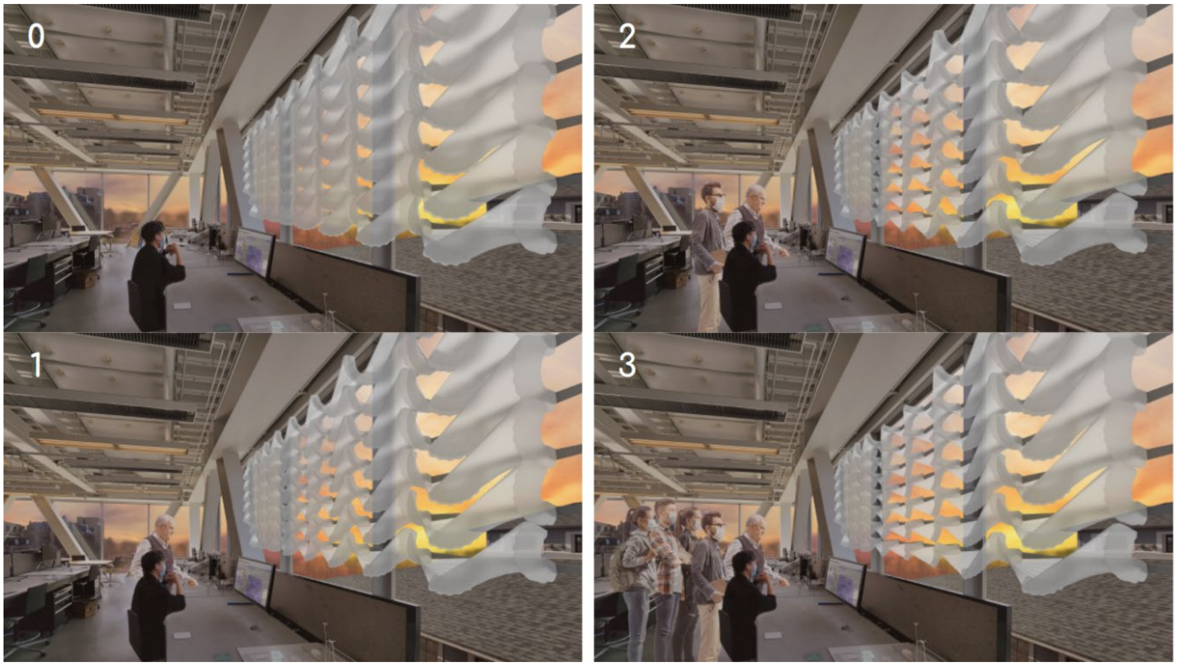


**Figure 47.** Design Speculation - Local Light Conditioning


**Figure 48.** Design Speculation – Social Distancing Alarm


**Figure 49.** Design Speculation – Health Habit Reminder

# CHAPTER 7

# RESULT

## *Introduction*

In this chapter, testing results from all four iterations of the study will be demonstrated and evaluated based on their respective difficulty of fabrication, performance (range of transformation), and application potentials.

## *Iteration One*

Among the four types of internal structural programming, serial channels were the most effective in generating both global deformation and local expansion differentiation **(Figure 50)**. However, despite the relative simplicity in their fabrication processes, the flap/pyramidal envelope profiles impose large restrictions in creating more complex shapes, making mold design rather challenging. In addition, these internal structures significantly constrained the expansion in both area and volume, making them a less appealing option for the shading/partition device designs.

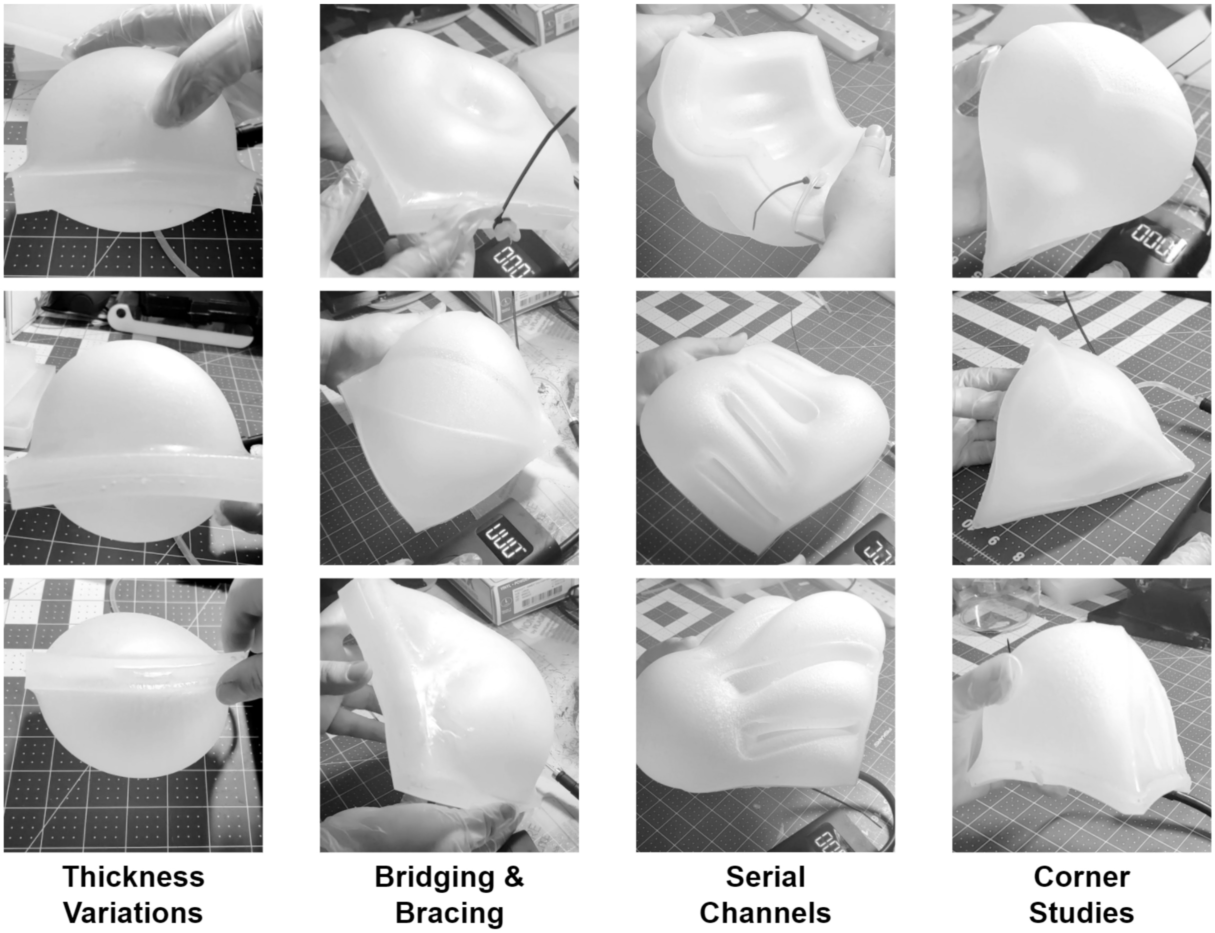


**Figure 50.** Testing Result - First Iteration

### *Iteration Two*

The second iteration using a segmented structure based on the actuator-membrane assembly gained a noticeable advantage in design flexibility **(Figure 51)** and scalability **(Figure 52)**. The poor performance and low consistency found in testing samples were primarily due to the choice of material and inadequate mold design. It must be noted that the actuator design that uses strain limiters to control its transformation is not the most efficient method compared to others adopted by locomotive soft robotic designs. However, the added benefit of larger actuator volume and visible tectonics makes it a better option for the particular application of shading/partition devices.

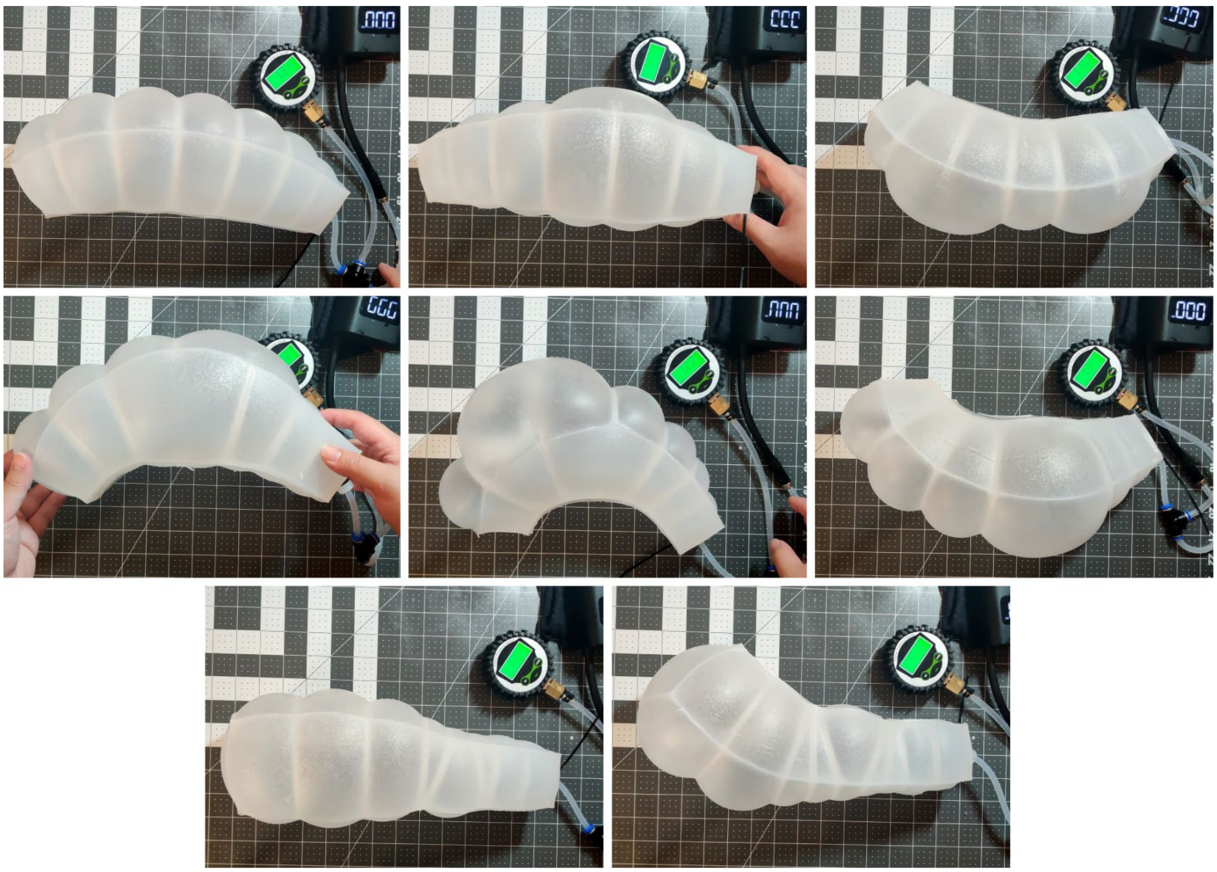

**Figure 51.** Actuator Testing Result - Second Iteration

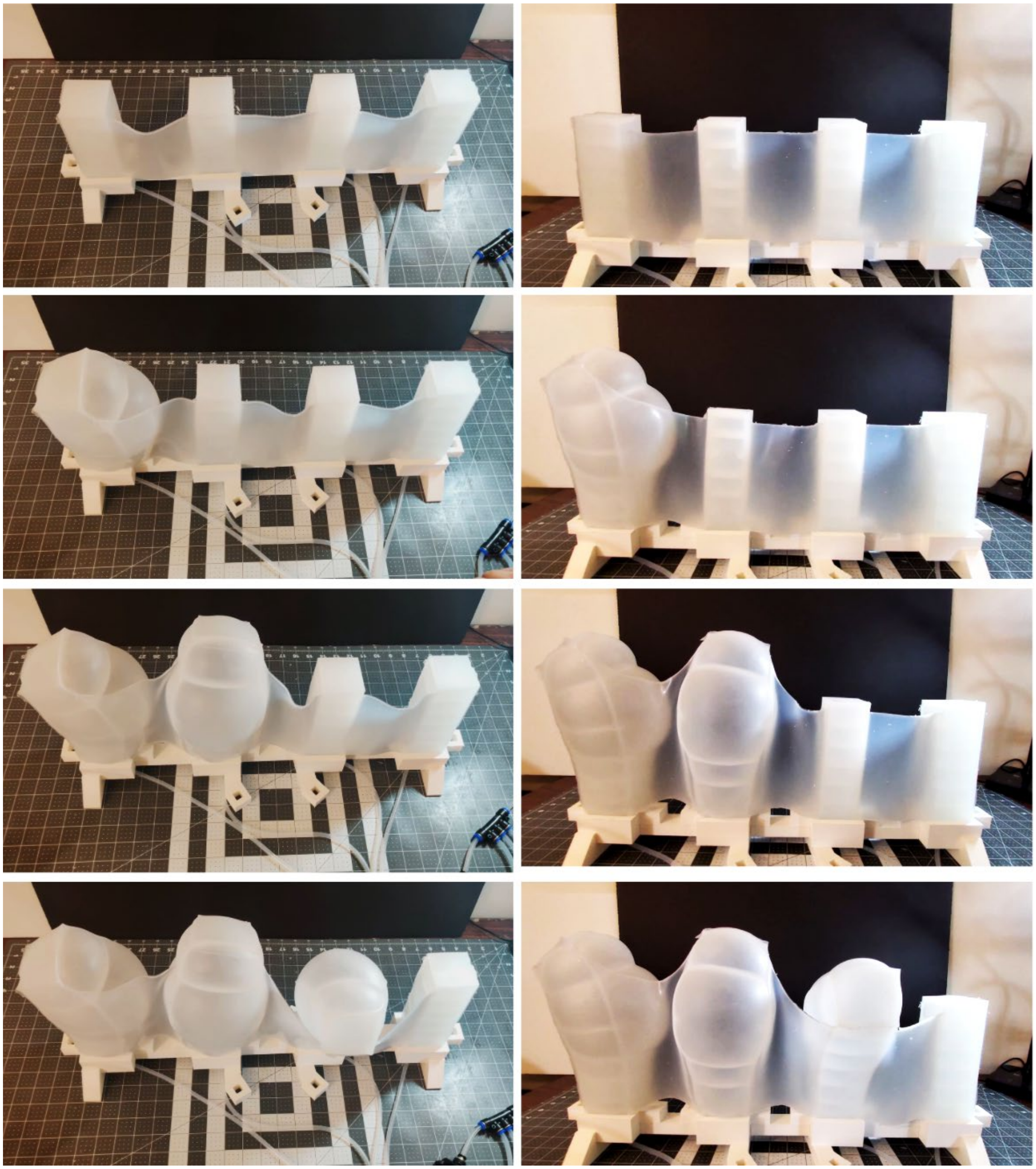

**Figure 52.** Assembly Testing Result - Second Iteration

### *Iteration Three*

The third iteration focused on improving the actuators' consistency and performance through material selection and mold design refinement. With these revisions, the new actuator samples finally met the expectation, and further structural explorations were conducted **(Figure 53)**. Despite the relatively demanding fabrication process, the usability of these actuators was largely enhanced. The examination of actuators directly placed on a LED panel also revealed the excellent potential for advancing the visual aspects of the device **(Figure 54)**. One minor issue was that delamination between the sidewall and strain limiters occasionally occurred at higher pressure levels.

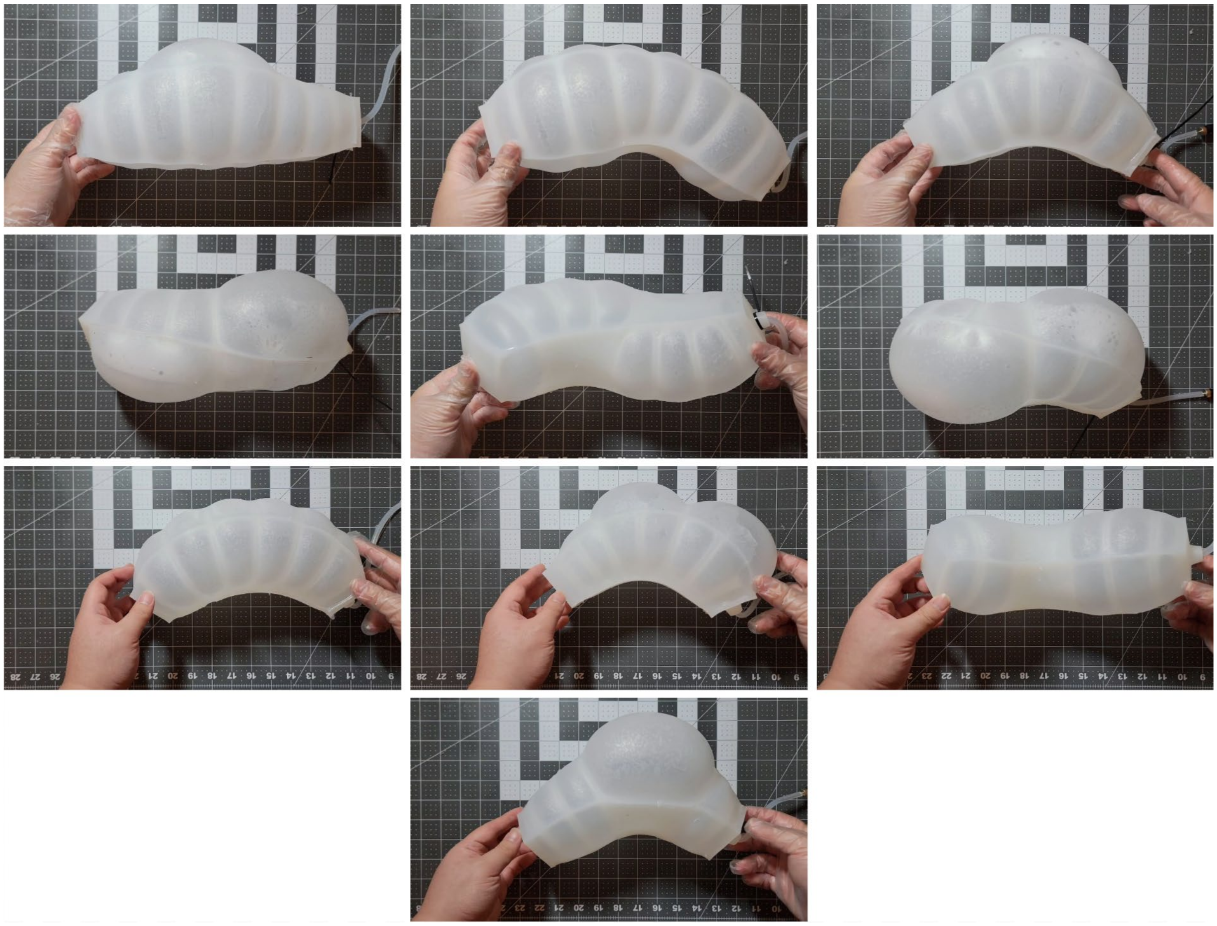

**Figure 53.** Actuator Testing Result - Third Iteration

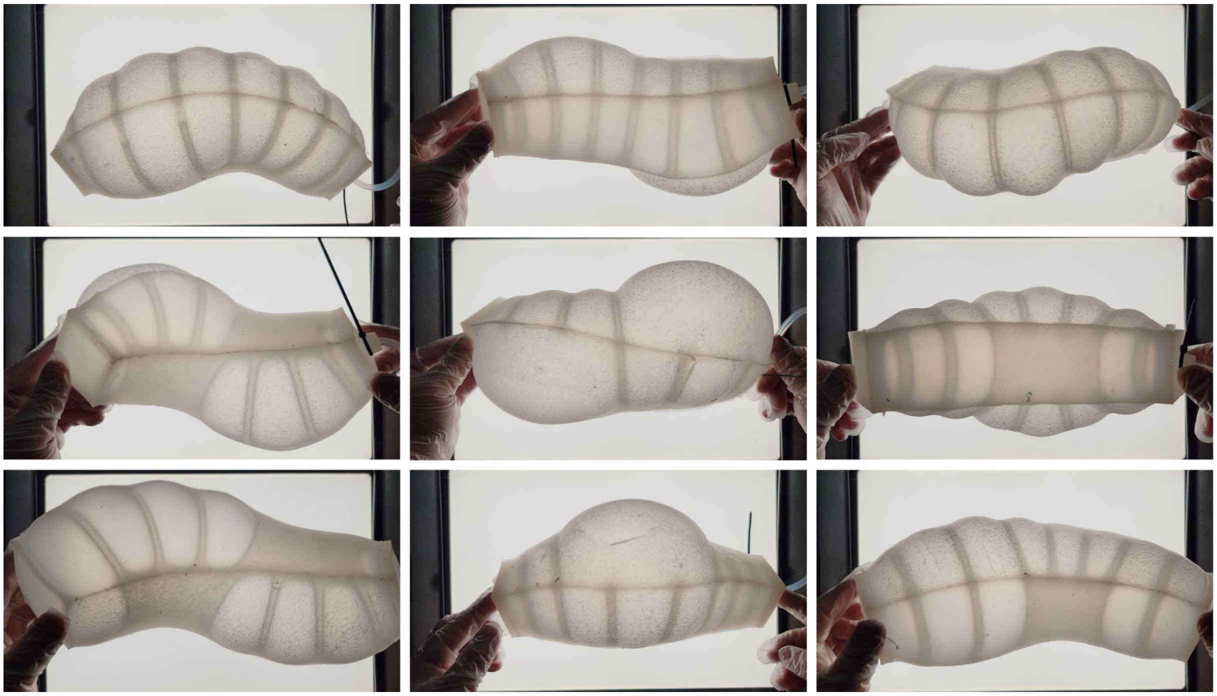

**Figure 54.** Actuator Examination - Third Iteration

The preliminary study on the membrane was less successful **(Figure 55)**. Although the fabrication was comparatively effortless, the performance was below expectation since it exhibited a negligible extension and exerted excessive stress on the actuators. However, this study indicated a set of parameters that needed revision towards the next iteration and good potential for application.

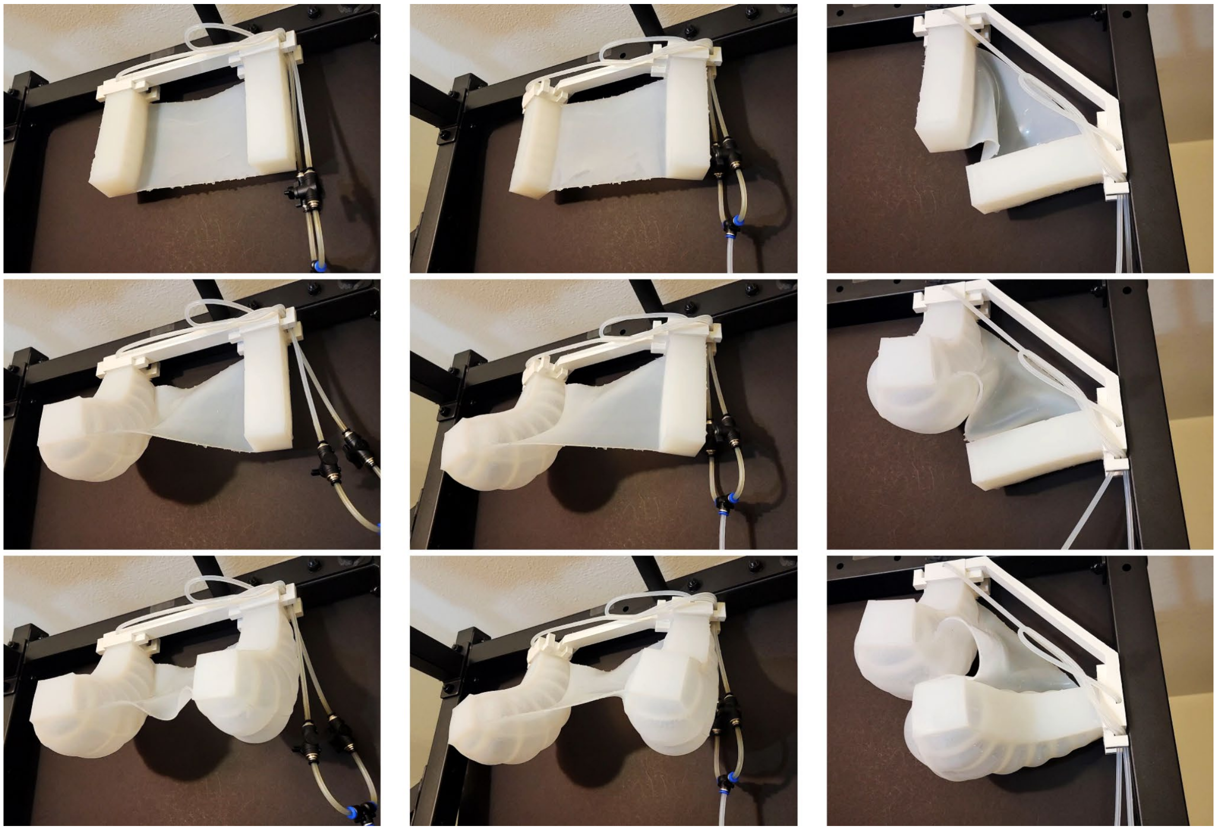

**Figure 55.** Assembly Testing Result - Third Iteration

### *Iteration Four*

The latest iteration solved the delamination issue that existed in the previous version of the actuator design by altering the profile of the strain limiters. The new design allows the actuator to be operated at a higher pressure level without tearing, thus enabling a more extensive range of transformations **(Figure 56)**.

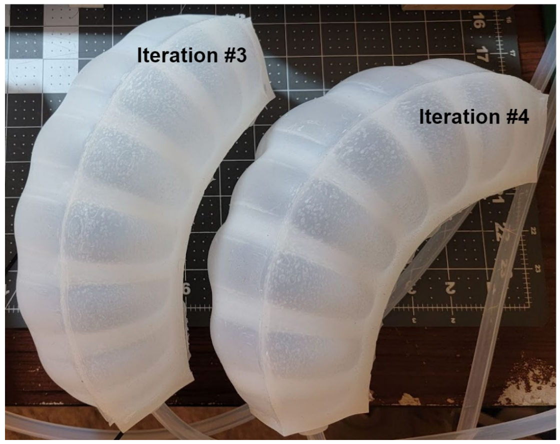


**Figure 56.** Actuator Design Improvement - Fourth Iteration

With the new mold design that can produce membranes of a significantly reduced thickness of 1.2mm, the assembly was finally able to perform adequately in the tasks it was designed for **(Figure 57)**. Resembling previous examination results of individual actuators’ capabilities of mediating light, the actuator-membrane system prototype exhibited unique light conditioning effects in several approaches. First, the transparency of the system increases upon air injection, which offers a great degree of control according to various lighting volume and intensity conditions. Second, the transformation in both area of coverage and bending angle of the assembly can be utilized to accommodate for changes in sun angles throughout the day. In addition, the changes in transparency and reflection also influence the visibility, providing additional privacy for indoor and outdoor uses.

Using the fully automated control platform with three interactive programs, the actuator-membrane assembly can now be employed for various environment conditioning requirements with sufficient flexibility in transformation control and functional customization **(Figure 58)**.


**Figure 57.** Assembly Testing Result - Fourth Iteration

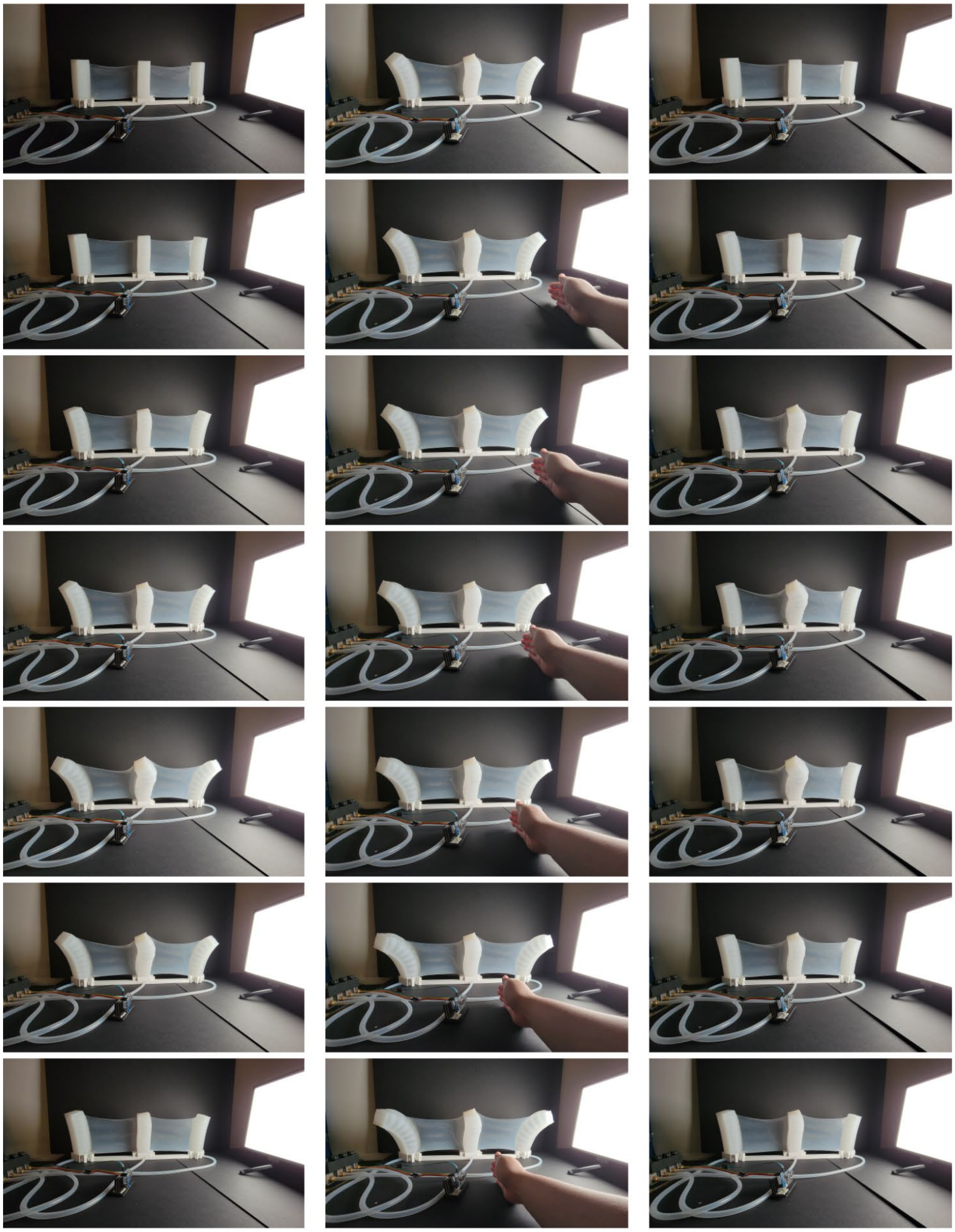

**Program 1**
**Light**

**Program 2**
**Light + Distance**

**Program 3**
**Light + Automatic Reciprocation**

**Figure 58.** Interaction Program Testing - Fourth Iteration

***Discussion***

Through the evolutionary process of developing and refining the actuator design, fabrication process, and interaction method, the design problem identified in the first chapter regarding costs, complexity of installation, and customizability of responsive shading devices can now be tentatively answered with the interactive prototype produced during the fourth iteration. The material cost of such a three-actuator-two-membrane assembly is under $30, and the universal structure enables a standardized manufacturing procedure in industrial settings, further reducing the initial cost. In addition, the modular construction allows convenient replacement at small scales without professional labor, leading to less maintenance cost in the long run. The result indicated the feasibility of using such a modular, responsive architectural device based on soft actuators and membranes for shading functions with a significantly simplified installation process and enhanced flexibility in user customization.

This research challenges the conventional use of inflatable structures in architectural applications, which mostly require inextensible materials and bespoke manufacturing processes. Through segmentation of larger architectural elements, the aggregable device using soft materials and standardized fabrication processes offered a cost-effective alternative method that is transportable, deployable, and customizable. Users can conveniently re-configure the device to fit the environment and their intended applications.

Although it was mentioned previously that the relative inefficiency of using strain limiters to control actuator transformation was less problematic considering the benefit of volume increase and visual tectonic presentation, the limited range of transformation still imposed constraints on both the performance and application potentials. However, materials that are more capable of this design could be utilized in further research or industrial settings so the device can sustain significantly higher pressure, thus increasing the upper limit of its range of transformation and durability.

The iterative design process, although productive, was limited by the lack of access to materials of higher performance and manufacturing facilities offering greater fabrication consistency. In addition, user feedback could have been invited early on to obtain insights into interaction designs and implementation strategies.

The prototype was only meant to demonstrate the functional viability of the design, so the integration of the control units and the development of a quick pneumatic connector were beyond the scope of this study. However, future research could consider real-life usability, which these subjects of studies may significantly enhance.

# CHAPTER 8

# CONCLUSION

This research aimed to identify effective design strategies for a responsive shading/partitioning device that is more cost-effective than existing design approaches and can be easily configured to accommodate the changing environment. Based on the result observed from the iterative design and prototyping process, it can be concluded that the aggregable unit featuring soft actuators and suspended membranes that transform under pneumatic pressure offered a feasible solution to this problem.

While using stretchable materials for the device imposed certain constraints on performance, especially in its area coverage and structural stability, when compared to existing designs that use tensile structure and inextensible films or fabrics, this approach provides new insights into how the “in-between state” from zero activation to full activation of such architectural devices can be utilized to create a continuous yet adaptive user experience. Although having less rigidity compared to a fully tensioned system, the all-soft construction offers greater flexibility in constrained spaces and safety in case of an accident. Moreover, the modular design approach allows users to fully customize the structure of the device assembly and the specification of interaction to program the transformation and functions based on their respective demands at affordable cost. By enabling customization, this approach would potentially result in significantly reduced cost in mass production.

Despite the inconsistencies among testing samples due to limited access to industrial-level materials and fabrication facilities, functions and features designed within the scope of this research mainly were achieved during the fourth iteration of design studies.

To better understand the implications of these results and further potential applications, future studies could improve materials and fabrication methods while addressing system integration design and usability studies.

## REFERENCES


1. Al Dakheel, Joud, and Kheira Tabet Aoul. "Building applications, opportunities and challenges of active shading systems: a state-of-the-art review." *Energies* 10.10 (2017): 1672.
2. Ye, Yunyang, et al. "Experimental study on the effectiveness of internal shading devices." *Energy and Buildings* 111 (2016): 154-163.
3. Sterk, Tristan d'Estrée. "Building upon Negroponte: a hybridized model of control suitable for responsive architecture." *Automation in construction* 14.2 (2005): 225-232.
4. Meagher, Mark. "Designing for change: The poetic potential of responsive architecture." *Frontiers of architectural Research* 4.2 (2015): 159-165.
5. Sterk, Tristan D. "Using actuated tensegrity structures to produce a responsive architecture." *ACADIA22 Conference 2003 Proceedings*. acadia, 2003.
6. Liu, Yudong, ed. *Defining Digital Architecture: 2001 Far East International Digital Architectural Design Award*. Birkhauser, 2002.
7. Diller, Elizabeth, Diana Murphy, and Ricardo Scofidio. *Blur: the making of nothing*. Harry N Abrams Incorporated, 2002.
8. Manzan, Marco, and Alberto Clarich. "FAST energy and daylight optimization of an office with fixed and movable shading devices." *Building and Environment* 113 (2017): 175-184.
9. Linn, Charles. *Kinetic architecture: design for active envelopes*. Images publishing, 2014.
10. Kensek, Karen, and Ryan Hansanuwat. "Environment control systems for sustainable design: a methodology for testing, simulating and comparing kinetic facade systems." *Journal of Creative Sustainable Architecture & Built Environment* 1.11 (2011): 27.
11. Krieg, Oliver David, et al. "HygroSkin–meteorosensitive pavilion." *Fabricate 2014 Conference Zurich*. 2014.
12. Spybroek, L., and B. Lootsma. "NOX–Aquatic Pavilion and Interactive Installation." *Neeltie Jans Holland, Domus* 349 (1997).
13. Burry, Jane, et al., eds. *Fabricate 2020*. UCL Press, 2020.
14. Wong, Nichol Long Hin, and Kristo Crolla. "Simplifying Catenary Wood Structures." (2019).

15. Schipper, H. R., and P. Eigenraam. "Mapping double-curved surfaces for production of precast concrete shell elements." *Heron* 61.3 (2016): 211.

16. Baranovskaya, Yuliya, Marshall Prado, Moritz Dörstelmann, and Achim Menges. "Knitflatable Architecture-Pneumatically Activated Preprogrammed Knitted Textiles." (2016).

17. Velikov, Kathy, Geoffrey Thun, and Mary O'Malley. "PneuSystems: cellular pneumatic envelope assemblies." (2014).

18. Wang, Adam, and Sean Ahlquist. "Pneumatic Textile System." (2016).

19. Souhail, Amir, and Passakorn Vessakosol. "PneuNets bending actuator design and fabrication using low cost silicones." *no. December* (2018).

20. Ilievski, Filip, Aaron D. Mazzeo, Robert F. Shepherd, Xin Chen, and George M. Whitesides. "Soft robotics for chemists." Angewandte Chemie 123, no. 8 (2011): 1930-1935.

21. Shepherd, Robert F., Filip Ilievski, Wonjae Choi, Stephen A. Morin, Adam A. Stokes, Aaron D. Mazzeo, Xin Chen, Michael Wang, and George M. Whitesides. "Multigait soft robot." Proceedings of the national academy of sciences 108, no. 51 (2011): 20400-20403.

22. Pikul, J. H., S. Li, H. Bai, R. T. Hanlon, I. Cohen, and Robert F. Shepherd. "Stretchable surfaces with programmable 3D texture morphing for synthetic camouflaging skins." Science 358, no. 6360 (2017): 210-214.

23. Moored, Keith W., et al. "Batoid fishes: inspiration for the next generation of underwater robots." *Marine Technology Society Journal* 45.4 (2011): 99-109.

24. Yan, Qin, Shiwu Zhang, and Jie Yang. "Initial implementation of basic actuated unit of a flexible pectoral fin driven by SMA." *2010 IEEE International Conference on Mechatronics and Automation*. IEEE, 2010.

25. Colorado, Julian, et al. "Biomechanics of smart wings in a bat robot: morphing wings using SMA actuators." *Bioinspiration & biomimetics* 7.3 (2012): 036006.